SCIENTIFIC COMMITTEE
ELEVENTH REGULAR SESSION

Pohnpei, Federated States of Micronesia
5-13 August 2015

SEAPODYM application for yellow tuna in the Pacific Ocean

WCPFC-SC11-2015/ EB-IP-01

I. Senina[1], P. Lehodey[1], B. Calmettes[1], S. Nicol[2], S. Caillot[2], J. Hampton[2] and P. Williams [2]

[1] Marine Ecosystems Modeling and Monitoring by Satellites, CLS, Satellite Oceanography Division. 8-10 rue Hermes, 31520 Ramonville, France
[2] Oceanic Fisheries Programme, SPC, BPD5, 98848 Nouma, New Caledonia

SEAPODYM application for yellowfin tuna in the Pacific Ocean.

Inna Senina[a] Patrick Lehodey[a] Beatriz Calmettes[a] Simon Nicol[b]
Sylvain Caillot[b] John Hampton[b] Peter Williams[b]

[a]Marine Ecosystems Modeling and Monitoring by Satellites, CLS, Satellite Oceanography Division. 8-10 rue Hermes, 31520 Ramonville, France
[b]Oceanic Fisheries Programme, SPC, BPD5, 98848 Nouma, New Caledonia

Contents

1 Executive Summary **3**
- 1.1 SEAPODYM v3.0 . . . 3
- 1.2 Environmental forcing . . . 4
- 1.3 Yellowfin tuna fisheries . . . 4
- 1.4 Main results . . . 5
- 1.5 Current and Future Work Plan . . . 9
- 1.6 Acknowledgments . . . 9

2 Introduction **10**

3 Background **10**
- 3.1 Biology . . . 10
- 3.2 Fisheries . . . 11

4 Data **12**
- 4.1 Fishing data . . . 12
- 4.2 Tagging data . . . 12

5 The model configuration **13**
- 5.1 Physical and biological forcing . . . 13
  - 5.1.1 ECCO reanalysis . . . 13
  - 5.1.2 INTERIM . . . 14
  - 5.1.3 Climate Change Projections . . . 14
- 5.2 Static model parameters . . . 14
- 5.3 Initial conditions . . . 15
- 5.4 Optimization . . . 15

6 Results **16**
- 6.1 Parameter estimates . . . 16
- 6.2 Validation . . . 19
- 6.3 Stock structure and size . . . 20
- 6.4 Impact of environmental variability . . . 20
- 6.5 Fishing impact . . . 21
- 6.6 Connectivity . . . 21
- 6.7 Climate change projections . . . 22

7 Tables **24**

8 Figures **30**

A Appendices **46**
- A.1 Seapodym fisheries . . . 46
- A.2 Fit to the catch and LF data . . . 46

References **63**

1 Executive Summary

SEAPODYM is a model developed for investigating spatiotemporal dynamics of fish populations under the influence of both fishing and environment. The model is based on advection-diffusion-reaction equations describing dynamic processes (spawning, movement, mortality), which are constrained by environmental data (temperature, currents, primary production and dissolved oxygen concentration) and distributions of mid-trophic (micronektonic tuna forage) functional groups. The model simulates tuna age-structured population dynamics with length and weight relationships obtained from independent studies. Different life stages are considered: larvae, juveniles, immature and mature adults. At larvae and juvenile phases fish drift with currents, later on they become autonomous, i.e., in addition to the currents velocities their movement has additional component linked to their size and the habitat quality. From the pre-defined age at first maturity fish start spawning and their displacements are controlled by a seasonal switch between feeding and spawning habitats, effective outside of the equatorial region where changes in the gradient of day length are marked enough and above a threshold value. The last age class is a "plus class" where all oldest individuals are accumulated. The model takes into account fishing and predicts total catch and size frequencies of catch by fishery when spatially distributed fishing data are available. A Maximum Likelihood Estimation approach is used to estimate model parameters. Conventional release-recapture tagging data were recently integrated within MLE to allow better observability of movement and habitat parameters.

1.1 SEAPODYM v3.0

Continuous development of SEAPODYM over the last three years contributed to a new version of SEAPODYM, referenced as 3.0, with major changes listed below:

1. Revision of the thermal preference function in the feeding habitat definition. Instead of Gaussian shape of thermal habitat function, a combination of sigmoid curves is used, which allows describing wider range of preferred temperatures and non-symmetric slopes.

2. One additional parameter associated to each functional group of prey can be estimated providing more flexibility in the representation of vertical behavior and access to tuna forage.

3. Revision of the spawning habitat with prey and predator functions defined separately (instead of using the prey-predator ratio as in previous version).

4. Implementation of alternative approach to account for fishing mortality and to predict catch without fishing effort, i.e. based on observed catch only, which can be particularly useful when reliable fishing effort is not available.

5. Growth-dependent computation of habitats and movement rates allowed significant improvement in terms of computational efficiency (20% decrease of computation time and 17% decrease of RAM use).

6. Function minimization can be set-up to include only conventional tagging data (in this case only tagged cohort will be modelled) or together with catch and length frequency of catch (full population mode).

7. Several additional diagnostic routines have been developed to facilitate the analysis and validation of simulation outputs.

1.2 Environmental forcing

The new long-term reference fits (1979-2012) are developed using a recent hindcast simulation INTERIM-NEMO-PISCES, hereafter INTERIM, prepared by the Institute of Research for the Development (O. Aumont, M. Dessert, T. Gorgues and C. Menkes). This simulation of the historical physical and biogeochemical ocean state is extended with several projections of potential climate change impact (see [Nicol et al, 2014]). However, the spatial resolution (2° refined in tropics to 0.5° in latitude) is too coarse to include tagging data in the optimization and a second configuration at 1° degree resolution (ECCO reanalysis) was used to run optimization experiments combining both fishing and tagging data.

1.3 Yellowfin tuna fisheries

The industrial fishing fleets targeting yellowfin comprise mainly three fishing gears - purse seine, long-line and pole-and-line (see [SPC Yearbook 2012]). Total annual catches by gear being used in the current SEAPODYM analyses are shown on Figure 1. Note that WCPO purse-seine data being provided and used in the current SEAPODYM configuration are not raised to the total catch representing between 60-75% of total landings during last two decades while long-line spatial dataset is complete (see Figure 2). In the EPO, the spatial catches correspond to the landings information only after 1998, showing some discrepancies in earlier years with the maximum mismatch being 33% of total catch in 1986.

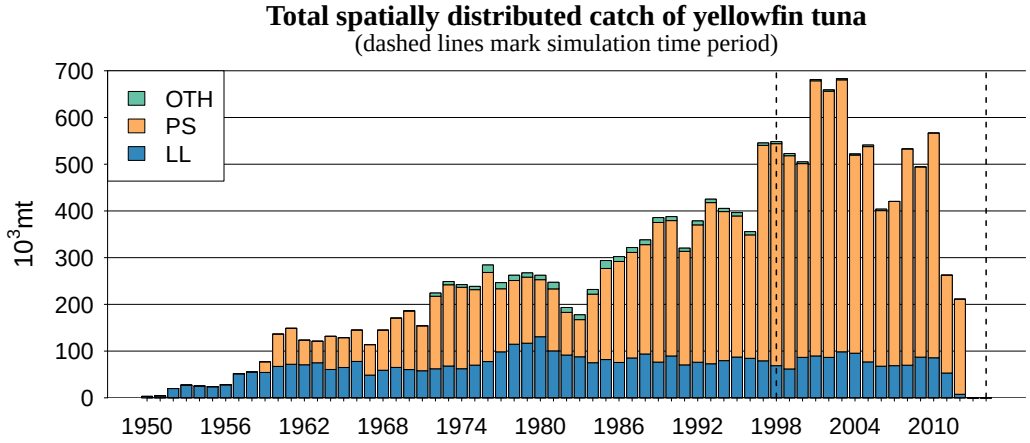

Figure 1: Total spatially-distributed catch of yellowfin population (Pacific-wide) being used in SEAPODYM analyses.

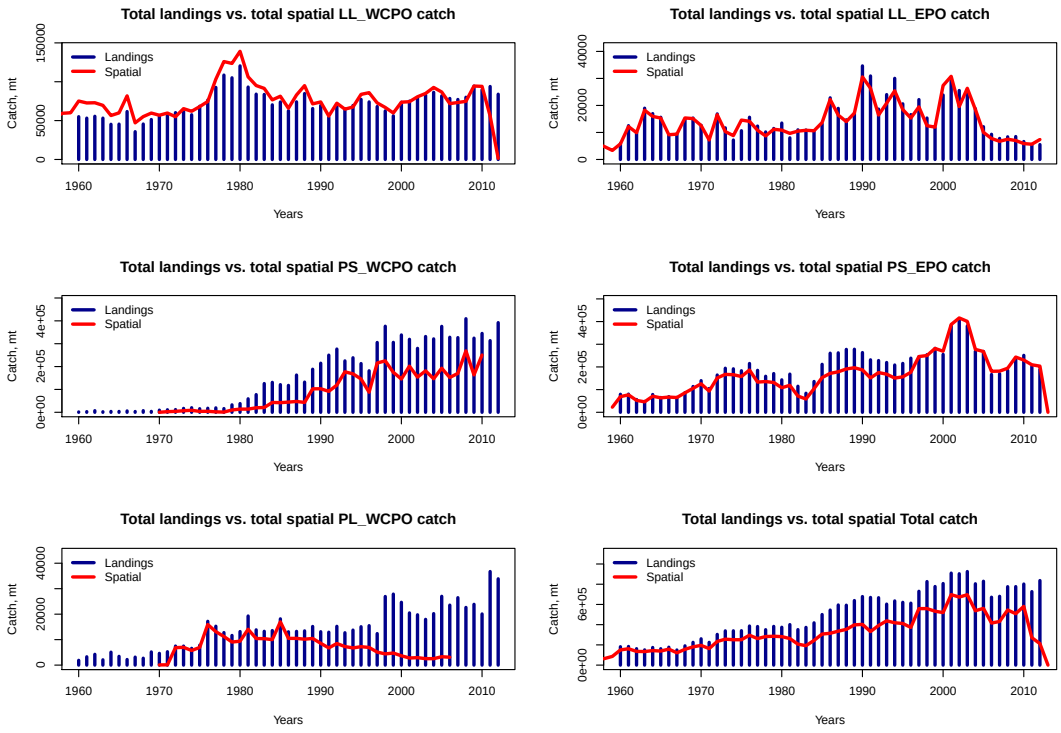

Figure 2: Comparison of total annual catches from spatial fishing dataset and from declared port landings (SPC Year Book, 2012). Note, some small discrepancies in long-line catches are due to conversion from number of fish to metric tons in spatial dataset.

1.4 Main results

1. The use of tagging and fishing data in an optimization experiment with a short 1° x 30 days ocean reanalysis time series (ECCO) allowed estimation of habitat and movement parameters within fixed a priori boundary values, suggesting low monthly advection values - between 0.35 BL/sec for the 3-month old and 0.04 BL/sec for the 7-year old cohort.

2. A new reference solution is provided with a 1° x 30 days long (1979-2010) hindcast simulation (INTERIM) optimized with fishing data only (see Figure 3).

3. With the revised definition of spawning habitat functions, the optimization suggested a much stronger response of the distribution of predators of larvae (micronekton) density leading to seasonal favorable "hot spots" for spawning in EPO (maximum in March -April), central Pacific (October-January), Bismarck Sea and north of PNG (beginning of third quarter) and in the north-west of East China Sea (spawning habitat picks in August-September).

4. The predicted oxygen concentration threshold value (0.24 ml/l) was estimated to a much lower level than measured lethal oxygen value. Thus, yellowfin abundance

distributions were predicted without constraint from dissolved oxygen concentration.

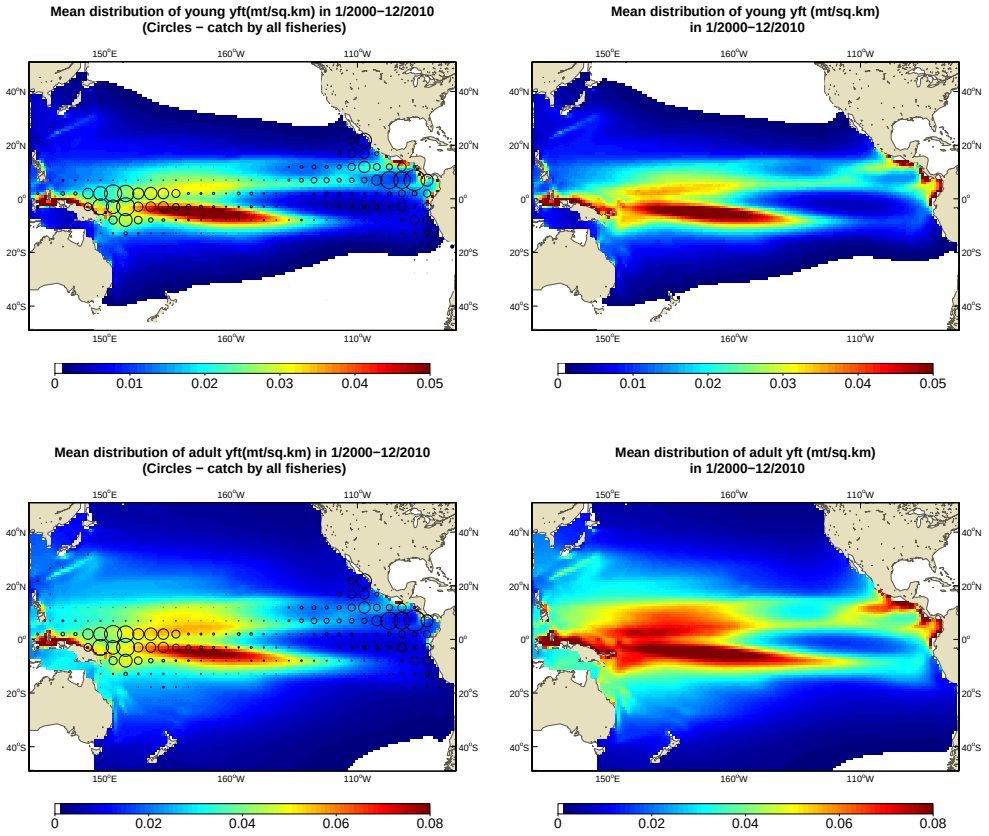

Figure 3: Average spatial distributions of young (top) and adult (bottom) biomass with (left) and without fishing (right).

5. Given the habitat variability the mean natural mortality rates were estimated between 0.05 and 0.19 mo^{-1}.

6. The spatial fit to observed catch was fairly good in the main fishing grounds, in particular the equatorial EPO but decreases towards the central gyre and higher latitudes where catch is generally occasional. The detail by fishery showed a difficulty to simulate the high variability observed in catch of tropical longline fisheries that are not targeting yellowfin. The fit is reasonable for all purse seine fisheries.

7. The detail by fishery showed a difficulty to simulate the high variability observed in catch of tropical longline fisheries that are not targeting yellowfin. The fit is reasonable for all purse seine fisheries.

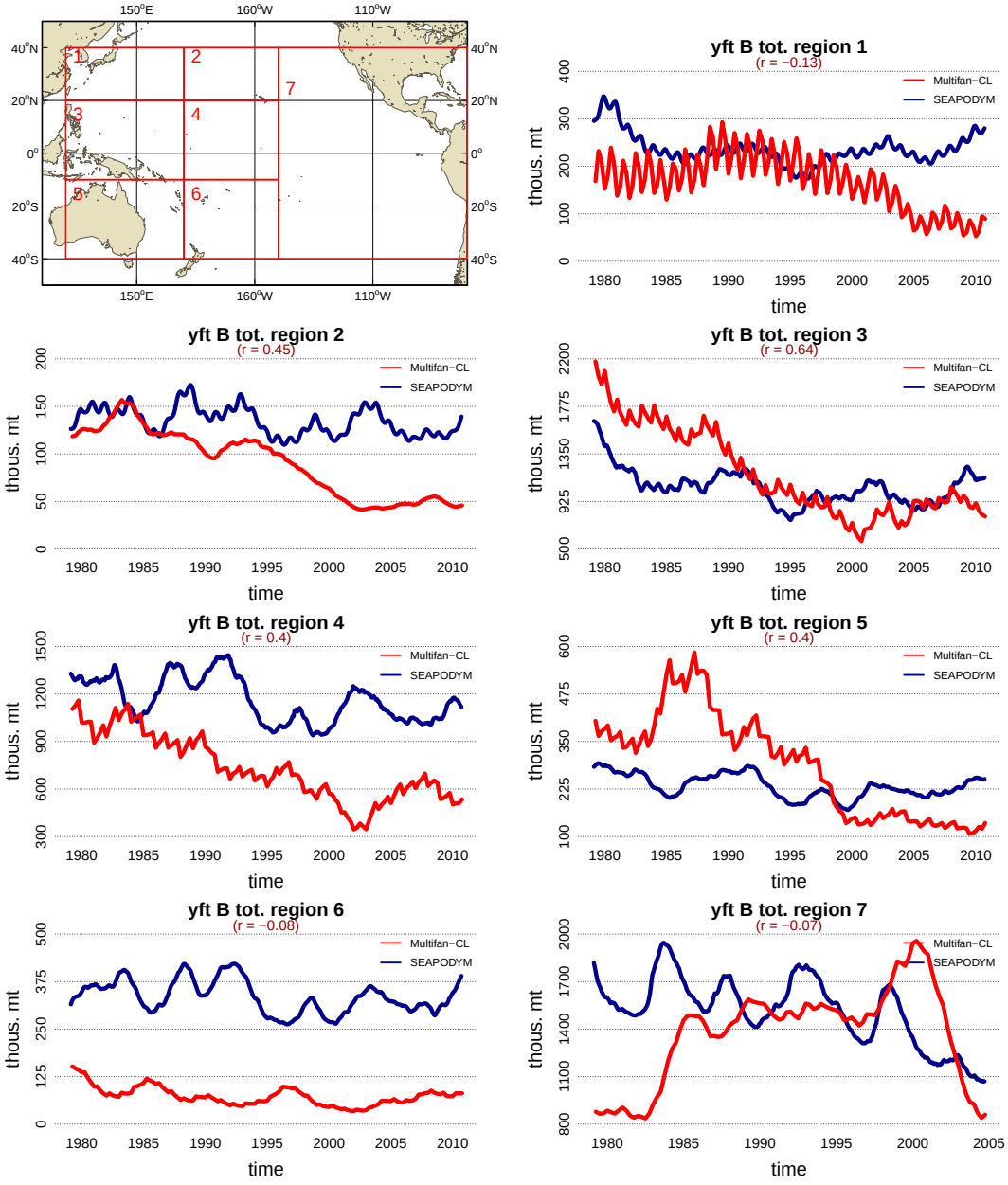

Figure 4: Regional comparison between SEAPODYM and Multifan-CL model predictions for total (immature and mature) biomass

8. EPO purse-seine catches associated with dolphin schools were systematically underestimated (positive error mean) and the errors increased during the years 2001-2003. Only, a 2-fold increase of catchability allowed decreasing the misfit during this period.

9. The overall fit to size frequencies samples are generally good with a few exceptions.

10. This model configuration and parameterization produced a biomass distribution

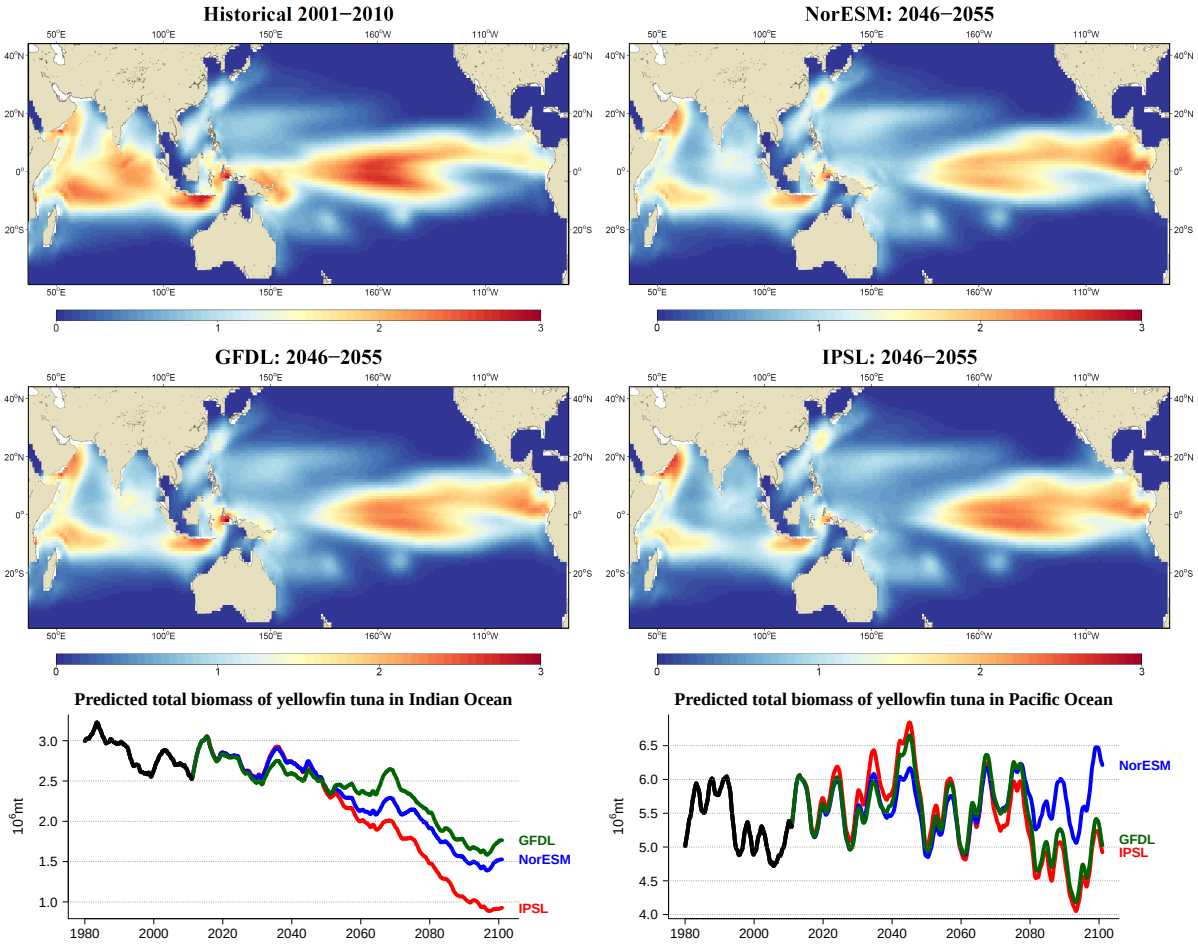

Figure 5: Historical mean (simulation with fishing) and projections of climate change impact (without fishing) on the distribution of yellowfin tuna larvae for the mid-century using atmospheric outputs from 3 different Earth Models under IPCC RCP8.5 scenario to drive the coupled physical-biogeochemical NEMO-PISCES model and then SEAPODYM.

with a core area associated to the warm waters of the warm pool and the warm currents moving north (Kuroshio), south (East Australian Current) and east (north equatorial counter current) with the extension of the biomass distribution towards sub-tropical areas and eastern Pacific (see Figure 3).

11. Excluding the Philippine-Indonesia region for which the coarse resolution and the lack of data produced strong uncertainty, the total biomass estimates converged relatively well with MFCL estimates, i.e., 2.5 - 4.0 Mt in the WCPO against 1.4-4.1 Mt for MFCL [Langley *et al.*, 2011], and 1.1-1.8 Mt in the EPO against 0.8-2 Mt estimated for MFCL by [Sibert *et al.*, 2006] (see Figure 4).

12. Keeping in mind that the geo-referenced dataset used for purse seine fisheries was incomplete in WCPO, the fishing impact was estimated to be 30% for adult biomass with local reduction exceeding 35% in warm-pool and up to 60% in EPO area.

13. Connectivity between Indonesia and PNG was investigated and indicated a slightly stronger connectivity from Indonesia to PNG (zero recruitment in Indonesia EEZ reduced adult biomass in PNG EEZ by 13.5%) than in the opposite way ("killing all recruits in PNG EEZ reduced adult biomass in Indonesia EEZ by 12.6%). However PNG EEZ contributes more adults to the rest of WCPO area (no recruitment in PNG EEZ results in 11.2% reduction of the rest of WCPO adult biomass while the absence of recruitment from Indonesia EEZ reduces the WCPO biomass only by 5.3%).

14. Climate change projections with no fishing scenario and three forcing datasets (IPSL, GFDL and NorESM) showed 1) the same long term decreasing trend in the Indian Ocean biomass after the mid-century, with the IPSL forcing leading to the largest decrease, the GFDL the smallest and the average climate driven reduction of 50%; 2) either no long term decline (NorESM) or a decrease arriving later after 2080 (IPSL, GFDL) for Pacific yellowfin biomass with clear eastward shift in the biomass distributions in all three simulations (see Figure 5).

1.5 Current and Future Work Plan

1. Fishing datasets need to be revised to raise the total of georeferenced catch data to 100% of nominal catch
2. ECCO 1° x 1 month with satellite-derived primary production forcing will be used with both tagging and catch data combined in the likelihood cost function.
3. Climate change projections will be completed and corrected from existing drift in the environmental forcings to provide an envelop of forecast.
4. The operational real-time global (1/4° x 1 week) and regional INDESO (1/12° x 1 day) models will be upgraded with the new SEAPODYM 3.0 after downscaling to target resolution and parameterizing the model according to achieved in this reference interim version.
5. Improvement of micronekton model (functional groups of prey for tuna) is continuing with acoustic data used for parameter optimization.
6. SEAPODYM documentation and website need to be updated.

1.6 Acknowledgments

The continued development and application of the SEAPODYM model to the work of the WCPFC Scientific Committee is facilitated through Project 62. The project affiliates the independently funded work on SEAPODYM into the SCs work programme. It is conducted in collaboration with the Oceanic Fisheries Programme (OFP) of the Secretariat of the Pacific Community. Project 62 is currently supported by Collecte Localisation Satellites and one project funded by the Government of Indonesia and the Agence Francaise de Dveloppement. The Inter American Tropical Tuna Commission has provided access to non-public domain data for the purposes of progressing the work programme of the WCPFC-SC.

2 Introduction

This paper presents an application of SEAPODYM to Pacific yellowfin tuna population (*Thunnus albacares*). It is based on the last SEAPODYM version 3.0 that includes several major changes detailed below. Compared to previous work [Lehodey *et al.*, 2009], the fishing data has been also fully revised and include more data at higher spatial resolution as well as additional size frequency data for the EPO fisheries provided by IATTC. The impact of revised habitat definition in SEAPODYM are first investigated using an environmental reanalysis ECCO-VGPM that is strongly constrained by ocean and satellite data but available only for the period 1998-2012. This study relies on optimization experiments with the large SPC conventional tagging data set, to check if these data can provide key information on both habitat preferences and movements. Then to estimate all model parameters an optimization experiment for the whole Pacific yellowfin tuna population and fisheries is conducted over a longer historical (but less realistic) simulation (1979-2010). Such long term optimization experiments are essential to estimate the parameters of the larvae-stock recruitment relationship. The fishing data and fisheries definition have been carefully revised before running this new model configuration. Once optimal parameterization is achieved, the model is used to investigate the connectivity in the western tropical Pacific between yellowfin tuna distributions in Indonesia and Papua New Guinea. Finally, preliminary results from first climate change projections under IPCC scenario RCP8.5 are presented. They are produced with environmental variables provided by the same coupled model, without fishing impact, and using three different atmospheric forcings; the objective being to increase the number of projections to provide an ensemble of simulations and thus to measure the uncertainty in the future trend of the yellowfin tuna population.

3 Background

3.1 Biology

Yellowfin tuna inhabit the tropical and sub-tropical waters of the Ocean. In the Pacific ocean, yellowfin tuna lifespan is estimated to be 9 years. Yellowfin are relatively fast growing fish reaching a length of about 140 cm at the age of 3 years (see e.g. [Lehodey and Leroy, 1999]) and maximal size of about 180cm. Previous studies on yellowfin growth showed different growth rates in different water masses, and two different growth periods seems to occur in the western central Pacific at least, with a slow down period for young fish (FL $<$ 60 cm) potentially due to the onset of first maturation. A consistent feature of all analyses of sex ratio is the rapid decline in the percentage of females at around 140 cm. Adult yellowfin become mature at the age of about 1.7 years, when they exceed the size of 100cm [Itano, 2000]. Spawning of yellowfin occurs in vast area of Pacific ocean being bounded in its northern and southern extremes by the 26°C surface isotherm [Lehodey and Leroy, 1999]. Based on tank experiments in the Panama Bight, Wexler et al (2011) established the optimal range of temperatures for rapid growth and moderate to high survival in first-feeding larvae from about 26°C to 31°C. While the occurrence of larvae is continuous across the equatorial Pacific within a zone approximately ten degrees north and south of the equator, three areas of higher larval density have been tentatively

recognized: 130-170°E, 180-160°W and east of 110°W.

Adult yellowfin can be found in water masses with a wide temperature range. Thus in the paper by [Boyce *et al.*, 2008] the authors suggest the optimal temperatures between 16°C and 28°C for yellowfin, which were derived from various published studies based on fishing, tagging and acoustic telemetry tracking data sources. The temperature preferences seem to define the vertical distribution of yellowfin. [Graham and Dickson, 2004] conclude that "yellowfin tunas prefer the range from 50 to 350m (15°C) but are also limited by the 3.5 ml/l oxygen barrier. However, [Brill, 1994] suggested that these tunas can support the oxygen levels as low as 1.9 ml/l indicating it is not limiting factor at these levels.

Horizontal movement rates vary among different areas of the Pacific ocean. Tagging studies show high site fidelity of yellowfin tuna in Baja California region (movement rates less than 1nmi/day, see [Schaefer *et al*, 2011]) while there were observed long-distance travels (more than 4000 nmi in six month) of yellowfin around Hawaiian Islands [Itano and Holland, 2000]. Modelling studies (e.g. [Sibert and Hampton, 2003], [Langley *et al.*, 2011]) provide estimates of horizontal movement rates for yellowfin, which are significantly lower than those for skipjack and bigeye, being between 0 and 0.3 BL/sec.

3.2 Fisheries

Two more or less independent stocks are proposed in the Pacific Ocean and managed by the WCPFC for the western Central Pacific area and the IATTC for the eastern Pacific area. The industrial fishing fleets targeting yellowfin comprise mainly three fishing gears - purse-seine, long-line and pole-and-line. There are some yellowfin catches by troll fisheries, but they account for about 0.5% of total catch yellowfin catches Pacific-wide [SPC Yearbook 2012].

After a regular increase associated with the development of equatorial purse seine fisheries in the 1980s and 1990s the total catch of yellowfin in the western central Pacific region has oscillated between 500 and 600 thousands metric tonnes (mt). Since late 1990s the purse-seine catch of yellowfin tuna has accounted for about 3-5 times the longline yellowfin catch and continues to diverge with longline catch ranging between 79,000-96,000 mt, which are below catches taken in the late 1970s to early 1980s (90,000-120,000 mt) [Williams and Terawasi, 2014]. In the eastern Pacific Ocean, the yellowfin catch peaked to above 400,000 mt during 2001-2003 but then declined below 200,000 mt in 2006 and since then vary in the range 200,000-250,000 mt (www.iattc.org). Large (adult) yellowfin are caught by longliners, while purse seiners and pole-and-line boats target both small (40- 60 cm FL) and large fish; the proportion of small fish being larger in the purse seine fishery using Fishing Aggregating Devices (FADs) or natural logs. Smaller fish (20-50 cm) are caught in large numbers by the domestic surface fisheries of the Philippines and Indonesia. The purse seine boats fishing on free schools in the WCPO experienced unusual catches of large (120-130 cm) yellowfin tuna in 2008, 2010 and 2012 [Williams and Terawasi, 2014] potentially associated with high recruitment years a few years before or/and due to increased catchability linked to favorable environmental conditions.

4 Data

4.1 Fishing data

Yellowfin tuna geo-referenced fishing data were provided by SPC and IATTC. Each fishery in SEAPODYM is defined with a single selectivity function and a catchability coefficient allowed linearly increasing or decreasing trend with time. Removing the fisherman-driven causes of changes in catchability, such as the change of target species or the fishing strategy, the remaining variability in catchability is driven by the spatial distribution associated with the environmental variability and fish movements, which are explicitly described by the model. Therefore it is critical to have a definition of homogeneous fisheries in terms of constant in space and time catchability and selectivity coefficients. The definition of fisheries for Pacific yellowfin tuna, which is assumed to satisfy to such criterion is provided in Table 1.

After combining the fishing data into the SEAPODYM fisheries (as shown in the Table reffisheries), a procedure for detecting outliers was applied within each fishery using the Hampel identifier rule for CPUE data. For each detected outlier, the effort was corrected based on the statistics of the seasonal CPUE in neighbouring areas. The catch was not modified with respect to the original data. Resulting catch and effort data distributions and time series are shown by fishery in Appendix A.1, Figure 30.

All long-line catch in this configuration have numbers of fish as a catch unit, while purse-seine and pole-and-line catch units are metric tons. Long-line data (catch and effort) are provided at a resolution of 5° x 5° x 1month while for surface gears (purse seine and pole-and-line) the resolution is 1° x 1° x 1month, excepted for Philippine and Indonesia fisheries.

The total annual catches from geo-referenced dataset built for SEAPODYM application were compared to the corresponding total annual nominal catch by gear (Figure 1. It appears that WCPO purse-seine catch data provided and used in the current SEAPODYM configuration represents between 60-75% of total landings during last two decades while long-line spatial dataset is complete (see Figure 2). In the EPO, the spatial catches correspond to the landings information only after 1998, showing some discrepancies in earlier years with the maximum mismatch being 33% of total catch in 1986. It is therefore important to keep in mind that model simulations did not account for the total fishing mortality. A complete geo-referenced dataset raised to the nominal catch level would need to be used in an update of this analysis.

Size frequency data provided by SCP (Pacific-wide long-line data and purse-seine in WCPO area) have variable resolutions ranging from 1° x 1° to 10° x 20°. In the EPO the size data are provided for purse-seine fleets over IATTC sampling regions (see http://www.iattc.org/Meetings2010/PDF/Aug/SAC-01-11-Port-sampling-program.pdf).

4.2 Tagging data

Both conventional and archival tagging data were used in the analysis of habitats and movements. The data from 30 archival tags were converted to monthly release-recapture type data hence resulting in 139 records during the period 2006-2014. Although the SPC tagging campaigns started in late seventies, due to the recent time period of ECCO-

VGPM dataset the release-recapture data starting 2008 were used in this analysis (see Figure 6)

5 The model configuration

5.1 Physical and biological forcing

SEAPODYM uses spatially explicit estimates of ocean and biological properties such as temperature, current speed, oxygen, phytoplankton concentration and euphotic depth from physical and biogeochemical ocean models to constrain tuna population dynamics. The outputs of SEAPODYM are therefore strongly dependent on the quality of its forcing.

The physical variables (temperature and currents) are outputs of ocean circulation models, either from hindcast simulations or reanalyses. They both provide the same outputs but in the first case the ocean model is forced by atmospheric variables (eg. surface winds) only. In reanalyses, the simulation also includes observations of oceanic variables (e.g. Argo profilers, satellite altimetry) that are assimilated in the model to correct the model and produce more realistic circulation patterns, especially at mesoscale resolution.

The biogeochemical variables (primary production, dissolved oxygen concentration and euphotic depth) can be obtained from a biogeochemical model that is coupled to the physical model or from satellite ocean color sensors from which chlorophyll-a, euphotic depth and vertically-integrated primary production are estimated. However, in that case the dissolved oxygen concentration is not available and needs to be replaced by a climatology (i.e., monthly average based on all available observations). All physical reanalyses are used with biogeochemical variables derived from satellite ocean color data.

All forcing variables are interpolated on the same regular grid and same time step prior to the use in SEAPODYM simulations. The mask is based on physical data availability at the levels of depth. The euphotic depth is used for averaging the physical data over three vertical layers: (1) Epipelagic layer, between the surface and 1.5 the euphotic depth (2) mesopelagic layer, between 1.5 and 4.5 the euphotic depth and (3) Bathypelagic layer, between 4.5 and 1.5 the euphotic level.

The configuration of current SEAPODYM application is summarized in Table 2. Each configuration refers to pre-processed dataset including physical, biochemical and biological variables listed in Table 2.

5.1.1 ECCO reanalysis

The physical model variables used in the ECCO configuration were provided by the ECCO Consortium for Estimating the Circulation and Climate of the Ocean funded by the National Oceanographic Partnership Program (http://www.ecco-group.org/). Original files with temperature and ocean currents datasets are in an irregular latitude grid and averaged by 10-day time step. The physical reanalysis is associated with the primary production and euphotic depth data derived from satellite ocean color data using the VGPM model and provided by Oregon State University (http://www.science.oregonstate.edu/ocean.productivity/index.php) with a 8-day x 1/12° resolution.

5.1.2 INTERIM

The INTERIM configuration (1979-2010) includes both physical and biogeochemical forcing provided by IRD: NEMO ocean model was coupled to the biogeochemical model PISCES (Pelagic Interaction Scheme for Carbon and Ecosystem Studies, Aumont and Bopp, 2006) at a coarse horizontal resolution of 2° (ORCA2 grid with a refined resolution of 0.5° in the equatorial band), see [Nicol et al, 2014]. It is forced by the ERA40-INTERIM atmospheric reanalysis (atmospheric temperature, zonal and meridional wind speeds, radiative heat fluxes, relative humidity, and precipitation) which has been corrected using satellite data (Dussin et al., 2013). Salinity, temperature and biogeochemical tracer concentrations (nitrate, phosphate, iron, silicate, alkalinity, dissolved oxygen and dissolved organic and inorganic carbon) were initialized from the World Ocean Atlas climatology (WOA09, Garcia et al., 2009), and model climatologies for iron and dissolved organic carbon. This simulation was produced for SPC by the French Institute for Research and Development [Nicol et al, 2014].

5.1.3 Climate Change Projections

Coupling ocean biogeochemistry with atmosphere-ocean models is expensive as is the optimization of SEAPODYM to numerous physical forcings of future climate. A pragmatic approach is developed (Nicol et al 2014) to produce an ensemble of simulation under IPCC scenarios based on a single physical forcing of the historical period (i.e., the INTERIM configuration above). SEAPODYM can then be optimized to this forcing which can then be used as the parameterizations for subsequent forecasts using each climate model. The NEMO ocean model (version 3.5) is forced with atmospheric trends extracted from coupled climate models for the RCP8.5 scenario [IPCC 2014] and coupled to the biogeochemical model PISCES (Pelagic Interaction Scheme for Carbon and Ecosystem Studies, Aumont and Bopp, 2006) following the same configuration used in INTERIM. With this method, the dynamic and biogeochemical state of the ocean for the 21st Century is simulated using atmospheric variables predicted from three Earth climate models involved in the Coupled Model Intercomparison Project Phase 5 (CMIP5). They are the IPSL, GFDL, and NorESM models. They all capture El Niño Southern Oscillation (ENSO) cycles in their simulation [Bellenger et al., 2013, Table 2].

5.2 Static model parameters

The yellowfin tuna population is structured into 61 monthly cohorts and a last "+ cohort" that accumulates fish older than 5 years, thus covering the age between 0 and 10 years maximum. The age at maturity occurs after 20 month, which corresponds to the length 107.6 cm. and weight 23.6 kg. Age-length and age-weight relationships are derived from the 2011 MULTIFAN-CL estimate [Langley *et al.*, 2011].

Two model parameters, namely the maximal predation mortality at age 0 and the Beverton-Holt stock-recruitment function coefficients were set constant in all optimization experiments and further in all simulations (see Table 3). Predation mortality parameter is often highly correlated with reproduction rate as they both act linearly on the local densities of the first cohort. The slope of Beverton-Holt function can only be estimated

using the long time series of model predictions in maximum likelihood framework thus covering several lifespans of the species.

5.3 Initial conditions

The INTERIM forcing (see Table 2) is available for the time period 1/1979-12/2010. The initial conditions for 1979 were obtained using the the SEAPODYM-NCEP 2° - 2-month age structure model (see [Lehodey et al, 2014]). In the optimization runs the first 5 years were however skipped in order to forget the initial conditions, thus only the data during the time period 1984-2010 were used to estimate the control parameters.

5.4 Optimization

ECCO. Two optimization experiments were conducted with ECCO forcing: E1) optimization of the complete model with fishing data (i.e., catch effort and size frequencies) and tagging data (both conventional and archival) and E2) optimization with tagging data and the model predicting the tagged cohorts only. In E1 experiments to reduce the impact of initial conditions on the parameter estimates, the first years of simulation are not included in the period of optimization starting in 2003. The end of the optimization period was constrained by the data availability and the amount of physical computer memory. Since after 2010 the fishing data seem to be incomplete (see Figure 2) and the conventional tagging dataset contains only few recaptures, the period of optimization was set to 2003-2010.

The new catch removal method to account for the fishing mortality independently of fishing effort and catchability was implemented and tested in this current optimization study. It consists in removal of the total catch by age directly from the cohort density simultaneously with the natural mortality and transport processes described by the model ADREs. Predicted catch is exactly the observed catch if the predicted local biomass by age is sufficient to sustain this level of catch. If it is not the case the predicted catch will be the total local available biomass (by age). Obviously, the use of such predictions in the likelihood allows observability of model parameters only in the grid cells where the predicted biomass is lower than the observed catch. This is a useful complementary approach to the first one predicting catch based on observed effort and catchability for which there are potentially many sources of uncertainty. The catch removal method was applied to the the purse seine fisheries while the effort and catchability method was still used for other (longline and pole-and line) fisheries. As usual, Philippine and Indonesia fishing data were not used in the optimization due to a lack of accuracy and catch was simply removed to account for fishing mortality.

We chose to apply catch removal method to purse seine fisheries due to the following properties of these data: 1) PS distributions are usually geographically localized (see Appendix A.1, Figs. 30) which give a weak signal to estimate the cohorts spatial distributions; 2) even though these fisheries use the same fishing gear and separated by the school flag, each of them represent the mix of data coming from different fleets, which might have different catchabilities; 3) the evaluation of the fishing effort is more problematic for the purse-seine than for the long-line gear as it is difficult to estimate the time of search and hence attribute it properly to the fishing effort.

To increase the fit with very high local catches, the catch removal method can lead to the tendency of the model to overestimate the biomass. To counterbalance this tendency, a prior information to constrain the average maximal stock value was added to the likelihood function. Several values were tested in the optimization experiments, including those estimated by Multifan-CL model [Langley et al., 2011], with the objective of finding the minimum value before the overall fit to data degrades quickly. The final experiment presented here was run with the a priori average total biomass =5,000,000 mt in the geographical box 120°E - 70°W; 35°S - 45°N during the period of optimization, i.e. 1984-2010.

The E2 experiments aimed to estimate only feeding habitat and movement parameters by fitting the observed distributions of recaptures resulted from the short and long-term displacements of tagged fish. The period of optimization in this case was set to three years, i.e. 2008-2010.

INTERIM. A revised definition of spawning habitat index was implemented in this analysis. This definition realises two separate mechanisms, which may influence the spawning habitat quality and hence the spawning success in the model. These are the food availability, the larvae predator (which are at the same time the food for the spawners) abundance. The new definition implies the use of three additional parameters, which were not yet estimated within MLE approach but calibrated through several optimization experiments (see final values in Table 3).

Since the ECCO model was optimized first with the aim to get the best fit based on complete dataset, including fishing and taggind data, the ECCO model configuration was used as an initial best guess in INTERIM optimization. Although INTERIM dataset was interpolated on 1-degree regular grid, to achieve maximal time period in optimization experiments the 2-degree INTERIM configuration was setup. The choice to cover several generations was made in order to improve the estimates of mortality and recruitment parameters. The tagging data were not included for two reasons: 1) the ORCA2 resolution is too low to predict the patchy distribution of tags; 2) we can use the knowledge obtained with ECCO forcing and tagging data. Hence, we'll rely on the ECCO estimates of habitat and movement parameters and allow only small variations of these parameters in the optimization with INTERIM. Thus, the first optimization phase was run with habitat and movement parameters being fixed. In terms of fisheries in the likelihood, three rounds of optimization runs were performed. In the first round we estimated the main demographic parameters using the catch, effort and LF data of long-line fisheries and only catch data (see ECCO report for more details about the method) of purse-seine fisheries. In the second round the feeding habitat and movement parameters were released. In the third round of optimization runs the catches of all fisheries were predicted based on the reported fishing effort and hence, purse-seine catchabilities were estimated. Finally, to provide the optimal solutions on 1-degree resolution, the model was optimized once to adjust model parameters to the INTERIM 1-degree dataset.

6 Results

6.1 Parameter estimates

ECCO. Estimated model parameters driving population dynamics are listed in the Ta-

ble 3. The fishing parameters are not shown. The optimal spawning temperature was estimated at its upper boundary value (32°C) with a standard error (2.89°C). Although these values appear to be high, the results of such parameterization is still consistent with the knowledge about the thermal preferences about spawners, namely that larvae mainly concentrate in waters with SST above 26°C while the high standard error makes the temperatures favorable up to 30-32°. According to the seasonal changes of the selected SST range and the availability of mature adults, the distributions of larvae density are variable with seasons, reaching the maximal densities in the warm-pool during 1-2 quarters while peaking in the sub-tropical waters (south of Kuroshio currents) and EPO area during the 3 quarter.

Following the work done for bigeye model with tagging data ([Lehodey et al, 2014]), six (by number of micronekton groups) new parameters were added to control the distribution of the feeding habitat. These parameters allow to modify the habitat index according to the weights to the micronekton groups (see parameters eFn in the Table 3). The optimal temperature for feeding habitat of adults was estimated and gives a thermal habitat decreasing with size/age from 21.5°C to 10°C. The estimated lower value (for the oldest fish) is out of the optimal range for yellowfin. The bias in the temperature estimate is likely related to the definition of the vertical layer over which the temperature is integrated (thus, the temperature of mesopelagic layer in the 5S-15N tropical band varies between 10°C and 15°C). So, the current temperature estimate increases the accessibility to the mesopelagic forage, which is then the one of the MTL groups with highest contribution to the habitat (Table 3). It is worth noting that the high contribution of bathypelagic forage to the habitat index is very localizes as the temperatures in bathypelagic layer are lower than 10°C everywhere except for the Kuroshio and Humbolt current systems.

The values of the oxygen function were both estimated at their lower boundaries resulting in no impact of oxygen levels in this configuration. This results may be attributed to the absence of a interannual variability in the oxygen fields due to the use of climatology and/or to the estimates of the thermal habitat, which assumes accessibility to mesopelagic layer with very low oxygen values.

However, the optimization experiments with tagging data only resulted in more realistic estimation of feeding habitat parameters. First, the temperature range 26.25-27.35°C provides very selective thermal habitat, which providing higher access to migrant micronektonic groups increases the accessibility to forage during the night in epi- and mesopelagic layers of warm-pool area. The thermal range 21.9-26.6°C for the large mature adult yellowfin is consistent with observations (see e.g. [Boyce *et al.*, 2008]). Unfortunately, although the oxygen function values are not estimated at their boundaries in this case, since the observed tagged fish is almost never recaptured in the waters with poor oxygen, the model is not sensitive to oxygen parameters and hence they cannot be well estimated.

The difference in estimates of movement parameters in the experiments with (E1) and without (E2) fishing data is also pronounced. Although in the experiments E1 all movement rates were estimated within their boundaries, thanks to the use of tagging data, the advection rate is an order of magnitude lower in E1 than in E2. The tagging data likelihood term allows estimating lower diffusion rates and improving advection rates through prediction of more realistic habitat gradients, however, the use of fishing data has

the opposite effect. Fitting catch (or CPUE) data always leads to the smoothed biomass distributions resulting from high diffusion and low advection rates. So, the final solution of E1 is balanced by maximizing these two likelihoods terms.

The mean natural mortality rates could be estimated in E1 experiments and they are between 0.07 and 0.22 mo-1 given the habitat variability. However, this results should be verified with longer INTERIM simulations in optimization, which may provide more reliable estimated of mortality rates.

INTERIM. All population model parameters are shown in the Table 3. The optimal spawning temperature was estimated at value 28.3°C) and a standard error was fixed to be 2.5°C as it tended to increase to its upper boundary in order to increase the density of the adult fish in the sub-tropical fishing ground. The rather strong response to the predators density (micronekton) in the spawning habitat index and a moderate effect of prey density (primary production) allowed to create the seasonal hot spots (see Fig. 8) in EPO (maximum in March -April), central Pacific (October-January), Bismarck Sea and north of PNG (beginning of third quarter) and in the north-west of East China Sea (spawning habitat picks in August-September). As a result larvae mainly concentrate in waters with SST between $25 - 31$°C (Fig. 7).

The new temperature function was tested in the latest ECCO experiments and current INTERIM configuration. Instead of Gaussian shape of thermal habitat function, we use the combination of sigmoid curves, which allows obtaining wider range of optimal temperatures and non-symmetric slopes. Given this function optimal temperature estimates (the temperatures at which the habitat index is greater than 0.5) vary between $25.6 - 31.8$°C for the youngest and $20.6 - 29.7$°C for the oldest cohort. The estimated preferred habitat temperatures by age, i.e. the average ambient temperatures computed given the density distribution of each cohort, are shown on Fig. 3.

The values of the oxygen function are still not satisfactory as the model critical oxygen value (0.24 ml/l) is much lower than lethal oxygen value. Hence, despite of the use of PISCES oxygen fields, the estimate is still biased. It is likely that the vertical structure being used in the current model configuration results in too low oxygen levels within the accessible layers. More work should be done to investigate the model sensitivity of parameter estimates to the vertical layer structure. The same problem with the estimates of eF_n, which control accessibility to the six micronekton groups. The changed drastically, diverging from the estimates of ECCO E2 experiments, finally implying the access only to epi and bathy-pelagic forage.

The advection rates were not allowed to vary far from the estimates of ECCO model optimization with the tagging data: the maximal advection rate is estimated on average about 0.35-0.065 BL/sec (Table 3) for youngest-oldest cohorts respectively. However, as the fit for the catch data was seriously deteriorated with low diffusion rates, the diffusion rates were estimated much higher, varying between 100-2000 nmi/day (Fig. 9).

The estimated theoretical mortality curve shows the decrease of monthly mortality rates from 0.1mo-1 (youngest, fixed) down to 0.03 mo-1 (about two years) and following increase up to 0.05 mo-1 for the oldest cohort. Given the habitat variability the mean natural mortality rates are estimated between 0.05 and 0.19 mo-1 (Fig. 9).

6.2 Validation

ECCO. The validation for tagging data fits is presented (see Figs. 10 and 11). Both experiments (E1 and E2, see the section 5 for details) show similar longitudinal and latitudinal extent of the predicted tag distributions. However, due to low advection rate and higher effective diffusion rates in response to generally lower habitat values in E1 solution its tagged density distributions are less heterogeneous that those of E2. The eastward movements observed in tagging data are realised with help of random displacements (diffusion), while E2 solutions with prevailed advection show no predicted tag recaptures east of 130W. Both solutions overestimate the meridional movements, but the fit is generally better with E2 (see meridional profiles on Figure 11). The overall fit of E2 solution is significantly better than E1, all three Taylor diagram validation scores (correlation, standardized variance, root-mean-squared-error) are better for E2 (0.91,0.69,0.32) than for E1 being (0.77,0.3,0.58).

As the objective to present ECCO experiments was to discuss the method and advances in the estimates of movement and habitat parameters with the use of tagging data, we will limit the discussion of ECCO model further, hereafter the results, obtained with INTERIM forcing will be presented and discussed.

INTERIM. The optimization results were validated using the whole time series, i.e. 1979-2012. The details of the model fit to catch and length-frequency data are shown on Figures 12, 13, 14 and in the Appendix A1 (Figs. 30 - 32).

The spatial fit to observed catch is fairly good in the main fishing grounds (R-squared goodness of fit values higher than 0.5 in tropical WCPO and about 0.8 in EPO), but decreasing towards the central gyre and higher latitudes where catch is represented only by long-line, where yellowfin is not a target species and yellowfin catches are occasional. Total catch is well predicted during the optimization period, however the EPO purse-seine catches associated with dolphin schools (see Figure 30, fishery S21) are systematically underestimated (positive error mean) and the errors increase during the years 2001-2003 (Fig. 14). Unfortunately, only the 2-fold increase (implemented) of S21 catchabilities during this period allows decrease of the misfit during this period, but no plausible reason can be found to justify such effort change except that it is not necessary for other EPO fisheries, which occur in the same fishing grounds.

The detail by fishery shows a difficulty to simulate the high variability observed in catch of tropical longline fisheries, e.g. L2 (Korea, Taiwan), L3 (China) and fisheries in which yellowfin is not a principal target throughout the year such as L7 (South Pacific, albacore target, being excluded from the likelihood), L9 (Australian coastal fleets, excluded from the likelihood), L10 (Hawaii) and L11 (targeting albacore and bluefin west of 145°E, excluded from the likelihood). The fit is reasonable for all purse seine fisheries, the lowest correlation being 0.67 and 0.66 for S20 (floating objects) and S22 (free schools). The overall fit to size frequencies samples are generally good (Fig. 32) with the exception of long-line fisheries L11 and purse seine fisheries S15 (WCPO, animal sets) and S18 (WCPO, free school sets) where a lot of smaller (S15) or larger (S18) size fish in observed catch are not predicted by the model. The opposite is shown for the EPO S21 fishery (dolphin schools), for which the model predicts the distribution shifted towards the larger fish size than observed, however the mean lengths in catch seem to fit rather well. The range of variability in predicted LF is always narrower than in the observation.

6.3 Stock structure and size

The overall estimates of reproduction and mortality parameters results in the following composition of yellowfin population in terms of total weight by life stage: about 0.1% of juveniles, 28% of young and 71.9% of adult biomass (see Figure 15). The predicted total stock fluctuates between 5.7 and 4.0 millions metric tons during the period 1980-2010 (Figure 16) with the maximum in the beginning of the time series and minimum in 2006. Note, that these figures were calculated excluding the area west of 120W, i.e. the Philippine-Indonesia regions for which the coarse resolution and lack of data produces high uncertainty.

Predicted biomass distribution shows a core area associated to the warm waters of the warm pool and central tropical part of the ocean (Figure 17). There are also moderate biomass levels in the warm currents moving north (Kuroshio) and south (East Australian Current) and low densities extending towards sub-tropical areas. Following the larvae distributions the recruitment of young population stages is more abundant in the WCPO, but occurs also in EPO area. High densities of young yellowfin are predicted in the eastern Pacific ocean (Peru and Costa Rica coastal current systems). The adult biomass in this region, is heavily depleted by fishing as seen on the right panel of Figure 17, showing locally a decrease of adult biomass above 50 or even 60% relatively to virgin biomass.

More detailed biomass estimates for WCPFC area are shown on plots comparing the SEAPODYM and Multifan-CL estimates (Figures 18 - 21). This INTERIM solution shows much closer match with MFCL predictions. In the WCPO the total biomass is between 2.5 and 4.0 Mt (against 1.4-4.1 Mt for MFCL [Langley *et al.*, 2011]).

In the EPO, if the first five years of the series are excluded, the predictions of the two models are even more close to Multifan-CL estimate [Sibert *et al.*, 2006] with biomass range for total biomass between 0.8-2Mt for Multifan CL and 1.1-1.8Mt for SEAPODYM.

6.4 Impact of environmental variability

Predicted spawning and larval recruitments conditions show seasonal and interannual variability. This signal frequency is smoothed and dumped while it combines with the internal dynamics processes of the species propagating towards the older cohorts (Figure 16). To illustrate the role of environmental variability on different life stages of yellowfin, the Hovmller diagrams with population densities were plotted for the tropical region (125E-75W; 10S-10N) and overlaid with Southern Oscillation Index (Figure 22).

It can be clearly seen that the spatial and temporal variability of yellowfin larvae is greatly influenced by ENSO cycles. The larvae distributions gets shifted towards the East during the El Niño episodes (1986-1987, 1991-1992, 1997-1998, 2002, 2004, 2009), at the same time increasing the recruitment success in the EPO. La Niña episodes, especially those occurred after strong El Niño (1989, 1999 and 2010) seem to create more favorable conditions for spawning and subsequent recruitment in young cohorts in the warm-pool. We note the remarkable increase in the densities of immature yellowfin on the west of 180E following the positive anomalies in SOI. The impact on the adult cohorts is less pronounced as the distributions reflect the outcome of both recruitment and movement processes. To trace the impact of environment on adult displacements, one can look at the dynamics of adult feeding habitat, which drives the adult movements and influences the local mortality rates. Indeed, it shows (lower right plot on the Figure 22) that the impact

of ENSO on adult's movements is similar to those on younger cohorts, i.e. inducing westward displacements during La Niña phases, which create more favorable habitat conditions in the Western Tropical Pacific and likely eastward movement during El Niño as the western habitats are no longer favorable and tuna will move to the East following the habitat gradients. It is interesting to note also that all peaks of total yellowin biomass observed during the simulation period 1979-2010 in both WCPO (namely 150E-150W) and EPO (see the Figure 23, curve without fishing) coincide with the negative ENSO phases.

6.5 Fishing impact

It is important to remind here that the incomplete purse-seine spatial dataset was used in this study, thus potentially leading to underestimation of fishing mortality. At basin-scale, and excluding the Philippines-Indonesia region, the fishing impact on yellowfin population is estimated to be 30% for adult biomass and maximum 9% for young biomass (Figure 23) associated with period of huge S21 catches in EPO. The spatial maps of fishing impact (Figure 24) show that locally the adult biomass reduction can exceed 35% in warm-pool and 60% in the most eastern region of the EPO. This result needs to be updated after revision of the geo-referenced fishing dataset.

6.6 Connectivity

While the Indonesia region is known to have important resource of yellowfin tuna, biomass in this region was not included in total Pacific biomass due to a large uncertainty based on both the coarse resolution used and the lack of reliable geo-referenced data to evaluate the model outputs in this region. It was interesting however to test the connectivity between this region and the rest of the Pacific, since connectivity is largely based on mechanisms independent of catch. The connectivity study consisted to run a reference simulation (without fishing) and then the simulations where all recruits (young or adult correspondingly) cohorts were "killed" in the model in the donor zone (i.e., here the Indonesian or Papua New Guinean EEZ). Then by measuring the change with the reference simulation we can quantify how much this donor zone contributes to the other region(s). The results of these experiments are presented in Table 4 for PNG as a donor area and Table 5 for Indonesian EEZ.

Connectivity measures indicate a slightly stronger connectivity from Indonesia to PNG (zero recruitment in Indonesia EEZ reduced adult biomass in PNG EEZ by 13.5%) than in the opposite way ("killing all recruits in PNG EEZ reduced adult biomass in Indonesia EEZ by 12.6%). However, Indonesian EEZ contributes much less biomass to the WCPO than PNG EEZ as only 5.3% of WCPO recruits and 8-9% of young and adult come from Indonesian EEZ while these percentages are 11.2% and 22-23% correspondingly for PNG EEZ. The total biomasses by life stages predicted by the model in the PNG and Indonesia EEZ are provided also in the Table 6.

6.7 Climate change projections

The Pacific INTERIM optimization was used to investigate the climate change impact (without fishing) over the 21st Century using three different projections achieved with the same RCP8.5 IPCC scenario (business as usual) but with atmospheric variables predicted from three Earth climate models: IPSL, GFDL, and NorESM. The model was run at global scale allowing to test if the parameterization achieved in the Pacific remains reasonably valid in the two other Oceans. In all cases, the simulations (without fishing) showed a distribution of yellowfin tuna in the Indian Ocean with large abundance in the equatorial western region that is likely overestimated given our knowledge mainly based on fisheries data. The simulations predicted also high biomass of adult along the coast of India and Indonesia that may be also overestimated. However, it should be noted that yellowfin catch data are under- or simply not reported by several important fisheries, in particular drift-nets from I.R. Iran and Pakistan, gill-net and long-line fishery of Sri Lanka, and coastal fisheries of Yemen, Oman, Comoros, Indonesia and India. Thus both our fishing data-based perception of the basin scale distribution and the current distribution after known and unknown intensive exploitation may be far from the state simulated here. Studies more focused on the Indian Ocean and including all historical tuna fisheries are necessary for a robust evaluation of the results in this region.

In the Atlantic Ocean, simulations predicted very low biomass of fish (Figure 25). A rapid analysis of the forcing variables demonstrated that the global coupled physical-biogeochemical model was not properly predicting the primary production in the Atlantic Ocean. Indeed, a comparison for the historical period with the primary production derived from ocean color in the equatorial region, where spawning of yellowfin tuna mainly occurs, indicates that in the Pacific and Indian Oceans, the model has a relatively constant bias that can be easily corrected through the optimization approach (Figure 26). However, in the Atlantic Ocean the bias is reversed and the strong seasonality is not well reproduced. The analysis was therefore concentrated on the Pacific and Indian oceans.

In the Indian Ocean, the three projections showed the same long term decreasing trend in biomass after the mid-century, with the IPSL forcing leading to the largest decrease and the GFDL the smallest. The decline is driven by temperature warming (Figure 27) as yellowfin reach the upper limit of its current favorable spawning temperature range in many places (with notable exception of Oman Sea area). Together with projected decrease in primary productivity(Figure 27), this leads to predicted decreasing trend in the stock at basin-scale with a climate driven reduction of 50% (Figure 28).

In average, the tropical Indian Ocean is warmer than Pacific and Atlantic Ocean by 2°C. The projected changes in the Pacific yellowfin biomass are different from the Indian with either no long term decline (NorESM) or a decrease arriving later after 2080 (IPSL, GFDL) (see Figure 28). However spatially the biomass is redistributed with a decrease in the west and an increase in central and eastern Pacific (Figure 29).

These first results are preliminary and did not account for a possible drift of the biogeochemical model that will be investigated using a reference control simulation. Then fishing scenarios will remain critical to predict the future trend of the stock.

List of Tables

1 Yellowfin Fishing Dataset 2014. Definition of SEAPODYM fisheries in Pacific Ocean. 24

2 Forcing variables used in current SEAPODYM application. Note that all variables were interpolated onto SEAPODYM grid with the resolution shown for micronekton variables. 25

3 Parameter estimates from three model configurations: ECCO1 - full model with both fishing and tagging data in the likelihood, ECCO2 - only tagged cohorts are modelled and tagging data likelihood is maximized and INTERIM refers to INTERIM-1degree model configuration. Parameters marked by asterisks were fixed in optimization experiment. Parameter with [or] were estimated at their lower or upper boundary correspondingly. The dash indicates that the parameter is not effective and could not be estimated. 26

4 Connectivity table for PNG EEZ as the donor area. The second column shows the percentages of PNG EEZ biomass of the corresponding age classes over WCPO biomass. The columns 3-5 provide the connectivity measures for three recipient areas, PNG EEZ, Indonesia EEZ and the rest of WCPO, that is the percentage reduction of adult biomass due to setting the biomass of a given population stage to zero in the donor area. Note, that all numbers are the average over the last five years of simulation, i.e. 1/2006 - 12/2010. 27

5 Connectivity table for Indonesian EEZ as the donor area. The second column shows the percentages of Indonesian EEZ biomass of the corresponding age classes over WCPO biomass. The columns 3-5 provide the connectivity measures for three recipient areas, PNG EEZ, Indonesia EEZ and the rest of WCPO, that is the percentage reduction of adult biomass due to setting the biomass of a given population stage to zero in the donor area. Note, that all numbers are the average over the last five years of simulation, i.e. 1/2006 - 12/2010. 27

6 Predicted averages by life stage with and without fishing for PNG and Indonesia EEZ calculated over 1/2006-12/2010 period. Recruits are quantified in mln. numbers, young and adult biomass is given in metric tons. . 27

7 Tables

Table 1: Yellowfin Fishing Dataset 2014. Definition of SEAPODYM fisheries in Pacific Ocean.

ID	Description	Nation	Resolution	Time period
L1	LL targeting BET and YFT	Japan	5°, month	1950 - 2011
L2	LL targeting BET and YFT	Korea, Chinese Taipei, Vanuatu	5°, month	1962 - 2011
L3	LL targeting BET and YFT	China	5°, month	1964 - 2011
L4	LL targeting BET and YFT	Chinese Taipei	5°, month	1958 - 2011
L5	LL targeting South Pacific Albacore: distant-water fleets	ALL	5°, month	1964 - 2012
L6	LL targeting North Pacific Albacore	Japan, Taiwan	5°, month	1952 - 2012
L7	LL targeting South Pacific Albacore	Pacific Islands	5°, month	1982 - 2012
L8	LL targeting BET and YFT	Pacific Islands	5°, month	1970 - 2012
L9	Longline Australia East Coast	Australia	5°, month	1985 - 2011
L10	Hawaii Longline	USA	5°, month	1991 -2011
L11	LL targeting Pacific Bluefin operating west of 145E	ALL	5°, month	1955 - 2011
L12	LL targeting BET and YFT	ID, ID-ID	5°, month	1958 - 2012
S13	PS sub-tropical	Japan	1°, month	1972 - 2008
S14	PS Anchored FADs, WCPO	ALL	1°, month	1979 - 2010
S15	PS Animal, WCPO	ALL	1°, month	1986 - 2010
S16	PS Drifting FADs, WCPO	ALL	1°, month	1982 - 2010
S17	PS Natural Fads, WCPO	ALL	1°, month	1979 - 2010
S18	PS Free swimming school, WCPO	ALL	1°, month	1979 - 2010
P19	PL WCPO	ALL	1°, month	1972 - 2008
S20	PS Floating objects	ALL	1°, month	1996 - 2013
S21	PS Animal, EPO	ALL	1°, month	1996 - 2013
S22	PS Free swimming school, EPO	ALL	1°, month	1996 - 2013

Table 2: Forcing variables used in current SEAPODYM application. Note that all variables were interpolated onto SEAPODYM grid with the resolution shown for micronekton variables.

Code	Variable	Description	Resolution	Time period
		Physical forcing		
ECCO	T, u, v	Ocean reanalysis with Kalman filter and adjoint assimilation schemes http://ecco.jpl.nasa.gov/	1°, 30 days	1/1998 -7/2014
NEMO	T, u, v	Ocean reanalysis, NEMO general circulation model with ERA-interim atmospheric forcing	ORCA2, 30 days	1/1979 -12/2010
		Biogeochemical forcing		
VGPM	PP, Z	Primary production and euphotic depth derived from ocean color http://www.science.oregonstate.edu/ocean.productivity	$\frac{1}{12}$°, 1 day	9/1997 -present
WOA	O_2	Levitus oxygen climatology	1°, 30 days	
PISCES	PP, Z, $O2$	Primary production, euphotic depth and oxygen predicted by PISCES model coupled to NEMO-INTERIM	ORCA2, 30 days	1/1979 -12/2010
		Biological forcing		
MTL	F	Six micronekton groups predicted by SEAPODYM-MTL model	1°, 30 days	1/1998 -7/2014
MTL	F	Six micronekton groups predicted by SEAPODYM-MTL model	1°, 30 days	1/1979 -12/2010

Table 3: Parameter estimates from three model configurations: ECCO1 - full model with both fishing and tagging data in the likelihood, ECCO2 - only tagged cohorts are modelled and tagging data likelihood is maximized and INTERIM refers to INTERIM-1degree model configuration. Parameters marked by asterisks were fixed in optimization experiment. Parameter with [or] were estimated at their lower or upper boundary correspondingly. The dash indicates that the parameter is not effective and could not be estimated.

$\boldsymbol{\theta}$	**Description**	**ECCO1**	**ECCO2**	**INTERIM**
	Reproduction			
σ_0	standard deviation in temperature Gaussian function at age 0, $^\circ C$	2.89	-	2.5*
$T_0^\star$	optimal surface temperature for larvae, $^\circ C$	32.0	-	28.26
α_P	prey encounter rate in Holling (type III) function, day^{-1}	-	-	2.0*
α_F	Gaussian mean parameter predator-dependent function, g/m^2	-	-	1.5*
β_F	Gaussian shape parameter in predator-dependent function	-	-	1.0*
R	reproduction rate in Beverton-Holt function, mo^{-1}	0.08	-	0.12
b	slope parameter in Beverton-Holt function, nb/km^2	10.0*	-	10.0*
	Mortality			
$\bar{m}_p$	predation mortality rate age age 0, mo^{-1}	0.1*	-	0.1*
β_p	slope coefficient in predation mortality	0.05	-	0.098
$\bar{m}_s$	senescence mortality rate at age 0, mo^{-1}	0.0002	-	0.00015
β_s	slope coefficient in senescence mortality	1.49	-	1.35
ϵ	variability of mortality rate with habitat index $M_H \in (\frac{M}{(1+\epsilon)}, M(1+\epsilon))$	1.25	-	3.135
	Habitat			
T_0	optimal temperature (if Gaussian function), or temperature range for the first young cohort, $^\circ C$	[21.5	26.25-27.35	25.62-31.75
T_K	optimal temperature (if Gaussian function), or temperature range for the oldest adult cohort, $^\circ C$	10.0	21.9-26.6	20.56-29.72
γ	slope coefficient in the function of oxygen)	[0	$6 \cdot 10^-4$	[0.0013
$\hat{O}$	threshold value of dissolved oxygen, ml/l	[0	0.21	0.24
eF_1	contribution of epipelagic forage to the habitat	$5 \cdot 10^-4$	[0	0.19
eF_2	contribution of mesopelagic forage to the habitat	1.46	[0	0.001
eF_3	contribution of migrant mesopelagic forage to the habitat	$2 \cdot 10^-4$	6.2	0.03
eF_4	contribution of bathypelagic forage to the habitat	1.4	[0	2.0
eF_5	contribution of migrant bathypelagic forage to the habitat	1.5	0.38	0.0
eF_6	contribution of highly migrant bathypelagic forage to the habitat	$1 \cdot 10^-4$	1.37	0.0
	Seasonality			
J_m	The midday of seasonal spawning migrations of adults, day	101	-	-
ρ_{cr}	Critical ratio of day to night length to mark spawning season	1.4]	-	-
	Movement			
V_m	maximal sustainable speed of tuna in body length, BL/sec	0.13	2.25]	[1.99
a_V	slope coefficient in allometric function for maximal speed	[0.1	[0.95	[0.95
σ	multiplier for the maximal diffusion rate	0.015	0.016	0.07]
c	coefficient of diffusion variability with habitat index	0.01	[0	0.3*

Table 4: Connectivity table for PNG EEZ as the donor area. The second column shows the percentages of PNG EEZ biomass of the corresponding age classes over WCPO biomass. The columns 3-5 provide the connectivity measures for three recipient areas, PNG EEZ, Indonesia EEZ and the rest of WCPO, that is the percentage reduction of adult biomass due to setting the biomass of a given population stage to zero in the donor area. Note, that all numbers are the average over the last five years of simulation, i.e. 1/2006 - 12/2010.

Ages	% of WCPO	Recipient area		
		PNG	Indonesia	Rest Of WCPO
Recruits	8.5	21.8	12.6	11.2
Young	8.0	48.6	22.0	22.3
Adult	6.1	81.7	21.7	23.6

Table 5: Connectivity table for Indonesian EEZ as the donor area. The second column shows the percentages of Indonesian EEZ biomass of the corresponding age classes over WCPO biomass. The columns 3-5 provide the connectivity measures for three recipient areas, PNG EEZ, Indonesia EEZ and the rest of WCPO, that is the percentage reduction of adult biomass due to setting the biomass of a given population stage to zero in the donor area. Note, that all numbers are the average over the last five years of simulation, i.e. 1/2006 - 12/2010.

Ages	% of WCPO	Recipient area		
		PNG	Indonesia	Rest Of WCPO
Recruits	16.6	13.5	40.7	5.3
Young	11.4	23.1	60.9	8.9
Adult	9.8	26.2	88.4	8.4

Table 6: Predicted averages by life stage with and without fishing for PNG and Indonesia EEZ calculated over 1/2006-12/2010 period. Recruits are quantified in mln. numbers, young and adult biomass is given in metric tons.

Area	**Fishing**	**Recruits**	**Young**	**Adult**
PNG EEZ	YES	4.5	67702	112352
	NO	4.6	82973	165642
Indonesian EEZ	YES	8.7	111776	229123
	NO	8.8	117153	263766

List of Figures

1 Total spatially-distributed catch of yellowfin population (Pacific-wide) being used in SEAPODYM analyses. 4
2 Comparison of total annual catches from spatial fishing dataset and from declared port landings (SPC Year Book, 2012). Note, some small discrepancies in long-line catches are due to conversion from number of fish to metric tons in spatial dataset. 5
3 Average spatial distributions of young (top) and adult (bottom) biomass with (left) and without fishing (right). 6
4 Regional comparison between SEAPODYM and Multifan-CL model predictions for total (immature and mature) biomass 7
5 Historical mean (simulation with fishing) and projections of climate change impact (without fishing) on the distribution of yellowfin tuna larvae for the mid-century using atmospheric outputs from 3 different Earth Models under IPCC RCP8.5 scenario to drive the coupled physical-biogeochemical NEMO-PISCES model and then SEAPODYM. 8
6 Conventional tagging data being used in optimization: (top) time at liberty histogram and time at liberty of the tags released at different time; (bottom) size distribution at release and recapture. 30
7 Predicted distribution of larvae at sea surface temperature 30
8 Predicted seasonal distributions of yellowfin larvae (decadal average). . . 31
9 Evolution of main model parameters through population life history: topleft - preferred habitat temperature; topright - average mortality rates; bottomleft - mean speed in body length and bottomright - mean diffusion rate 31
10 Maps of observed (top) and predicted by SEAPODYM-ECCO tag recapturesas a result of E1 (full likelihood) and E2 (only tagging data likelihood) optimization experiments over the period 2008-2010. The red circles show the release positions. 32
11 Comparison of observed and predicted tag recapture distributions: (top) longitudinal and (bottom) latitudinal profiles. Red dots show the number of releases. On the left - the result of full likelihood estimation, on the right - only tagging data in the likelihood. 33
12 Spatial map of validation metrics: (left) R-squared goodness of fit and (right) squared Pearson correlation coefficient. 33
13 Taylor diagram, providing three aggregated metrics of model fit to the data: standard deviation (distance from (0,0) point depicts the ration between model and data standard deviation), correlation (angular coordinates) and normalized mean squared error (concentric circles with the green bullet being the center) 34
14 Monthly time series of total observed and predicted catch (left) and CPUE (right) with their standardized residuals 34
15 Population composition by life stage 35
16 Time series of (from top to bottom) Larvae, young, adult and total biomass 35

17 Average spatial distributions of (from top to bottom) young, adult and total biomass with (left) and without fishing (right) 36
18 Regional comparison between SEAPODYM and Multifan-CL model predictions for recruitment 37
19 Regional comparison between SEAPODYM and Multifan-CL model predictions for spawning biomass 38
21 Comparison of (from top to bottom) recruitment, spawning and total biomass predicted by SEAPODYM and Multifan-CL models for WCPO (left) and EPO (right) (immature and mature) biomass 40
22 Variability of tropical (average over 10°S-10°N) biomass of larvae, and young and adult yellowfin and adult (3-yr old) habitat and Southern Oscillation Index (axis on the top of the map). 41
23 Quantification of fishing impact on young and adult population stages . . 42
24 Spatial fishing impact on young and adult population stages. Contour lines show the index $\frac{B_{F0}-B_{ref}}{B_{F0}}$ and colour shows the average biomass reduction due to fishing. 42
25 Snapshot of the total biomass of yellowfin tuna at the peak of El Niño episode in January 1998. 43
26 Comparison of primary production means predicted by INTERIM and estimated from satellite ocean color and VGPM model for three oceans. . 43
27 Percentage changes in Primary Production and SST variables predicted by INTERIM with NorESM, IPSL and GFDL forcing under IPCC RCP8.5 scenario. 43
28 Predicted total biomass (historical simulation with fishing) and projected (without fishing) impact of climate change using atmospheric outputs from 3 different Earth Models under IPCC RCP8.5 scenario to drive the coupled physical-biogeochemical NEMO-PISCES model and then SEAPODYM. 44
29 Larvae (top) in Nb/sq.km and adult (bottom) in mt/sq.km distributions of yellowfin tuna predicted with INTERIM historical (2001-2010) and 3 different future climate forcings from 3 Earth Models under IPCC RCP8.5 scenario. 45
31 Monthly time series of observed and predicted catch by fishery 55
32 Observed (grey) and predicted (red) length frequencies distribution and mean length in catches. 59

8 Figures

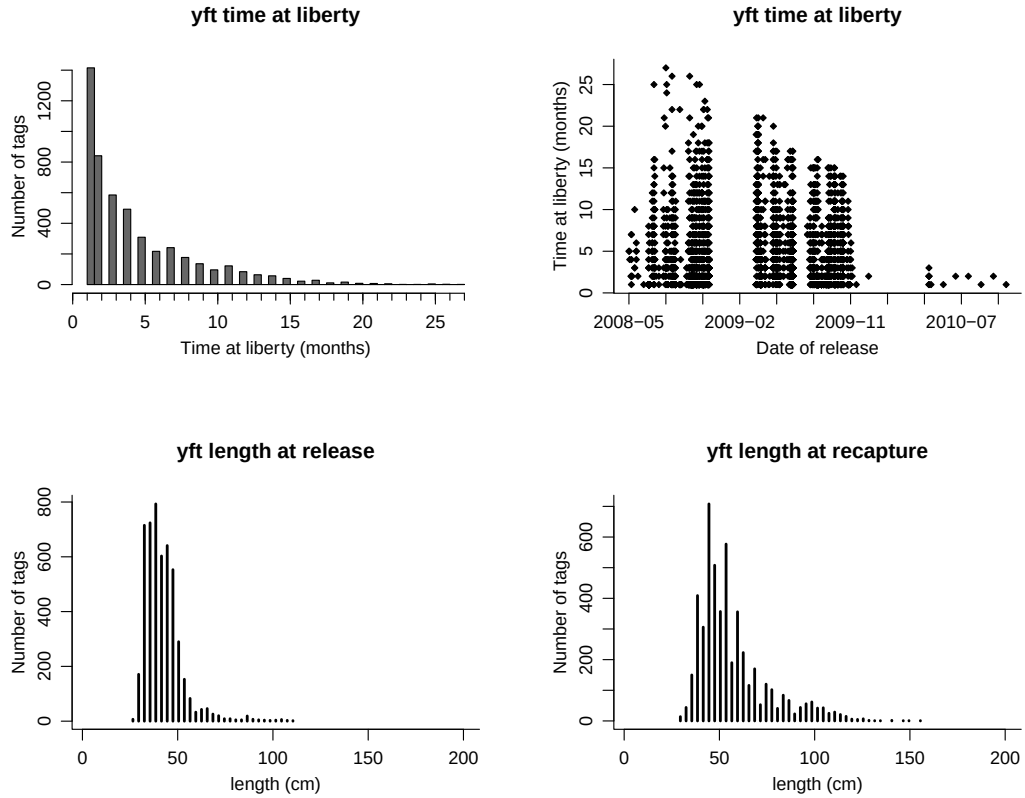

Figure 6: Conventional tagging data being used in optimization: (top) time at liberty histogram and time at liberty of the tags released at different time; (bottom) size distribution at release and recapture.

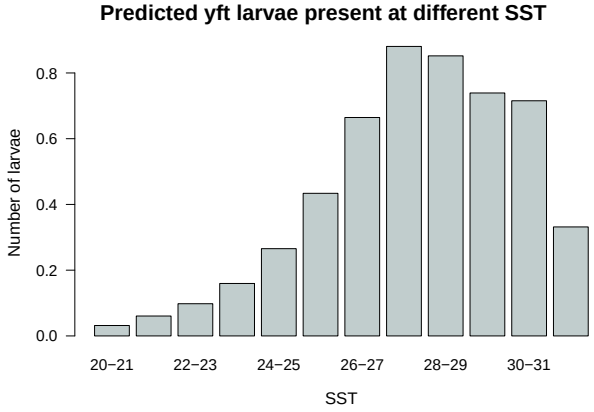

Figure 7: Predicted distribution of larvae at sea surface temperature

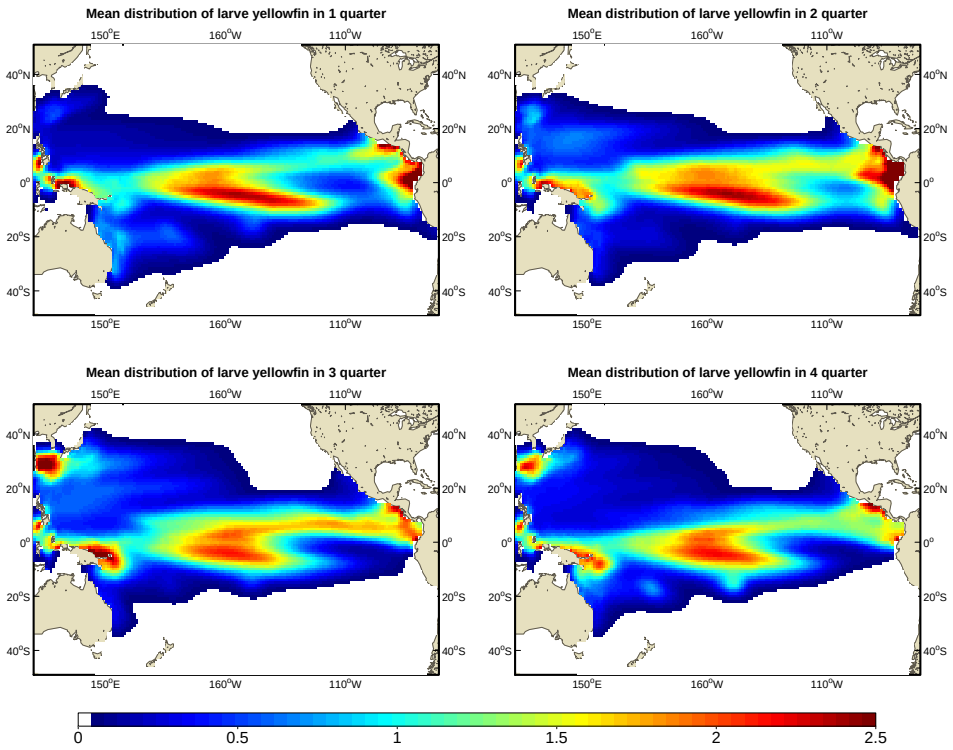

Figure 8: Predicted seasonal distributions of yellowfin larvae (decadal average).

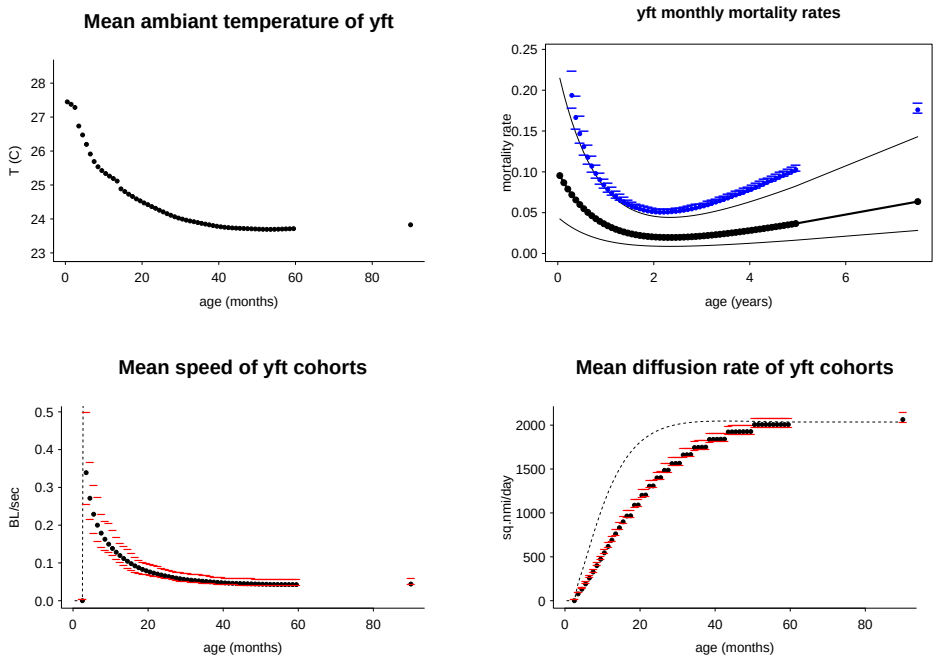

Figure 9: Evolution of main model parameters through population life history: topleft - preferred habitat temperature; topright - average mortality rates; bottomleft - mean speed in body length and bottomright - mean diffusion rate

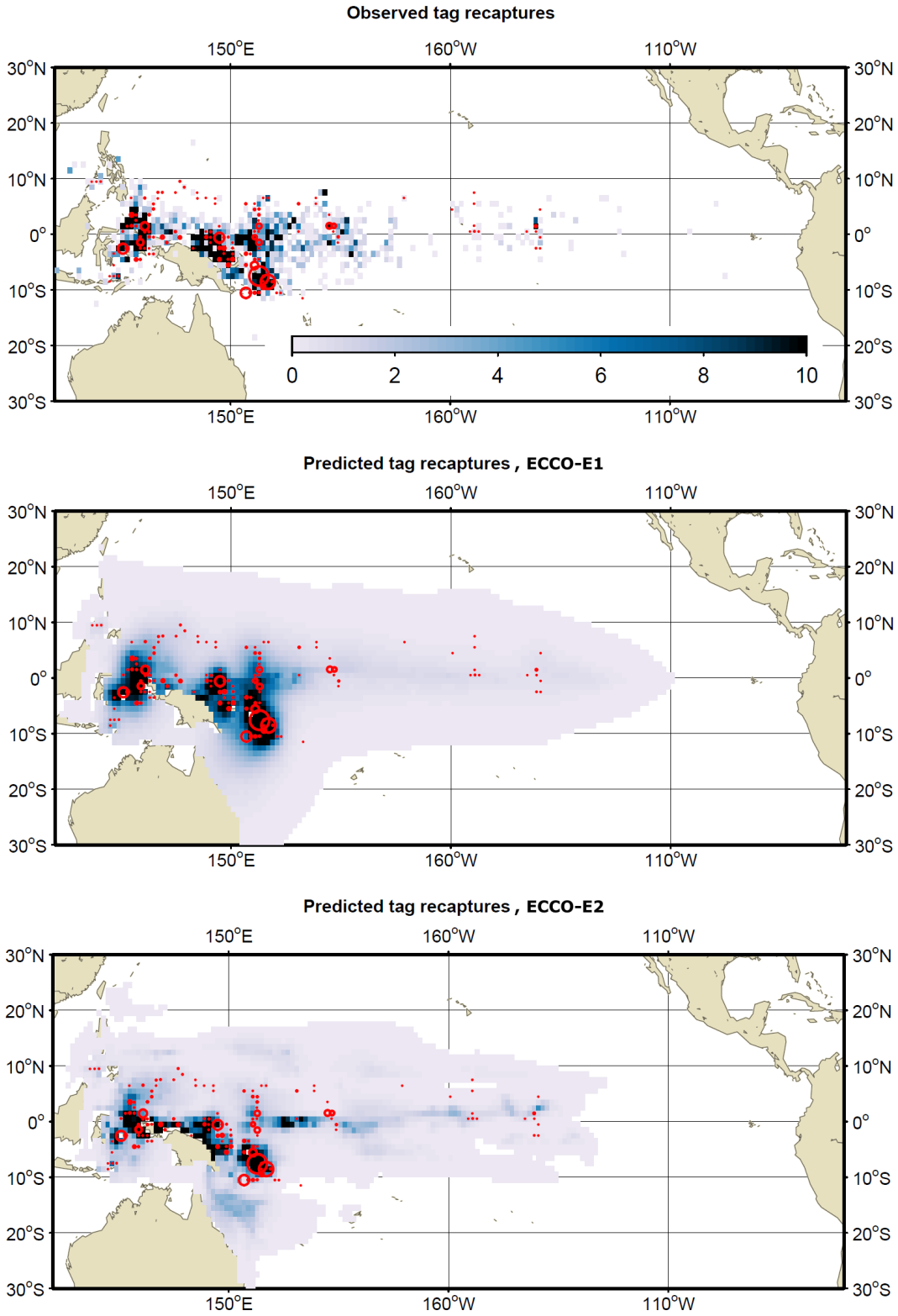

Figure 10: Maps of observed (top) and predicted by SEAPODYM-ECCO tag recapture-sas a result of E1 (full likelihood) and E2 (only tagging data likelihood) optimization experiments over the period 2008-2010. The red circles show the release positions.

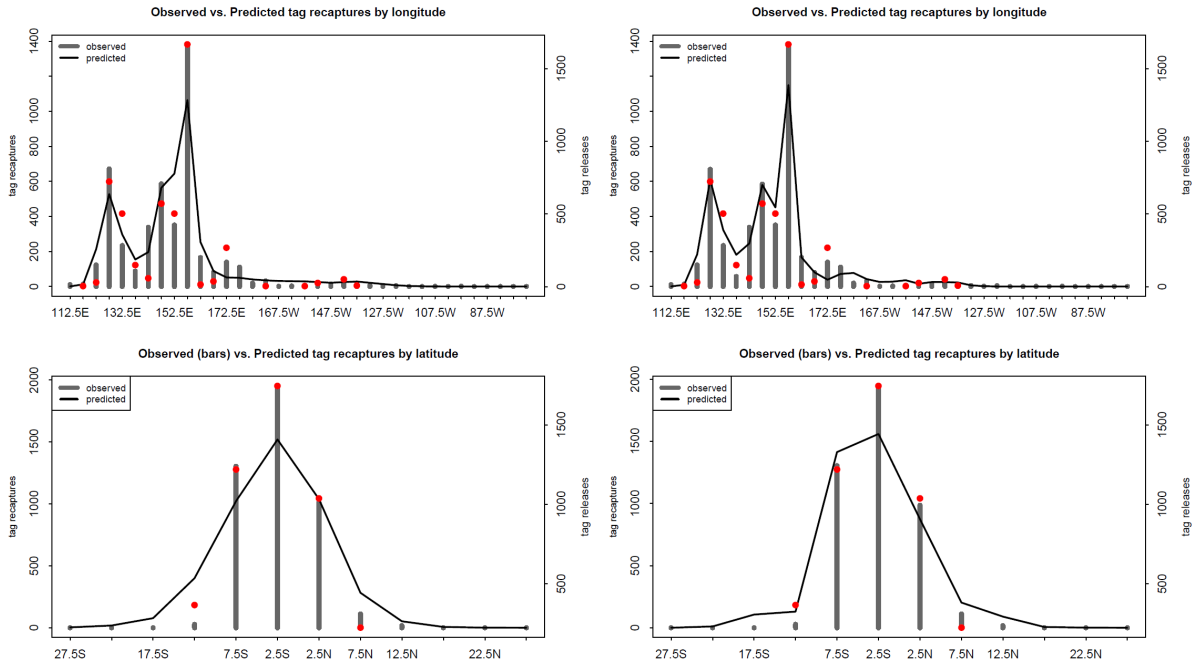

Figure 11: Comparison of observed and predicted tag recapture distributions: (top) longitudinal and (bottom) latitudinal profiles. Red dots show the number of releases. On the left - the result of full likelihood estimation, on the right - only tagging data in the likelihood.

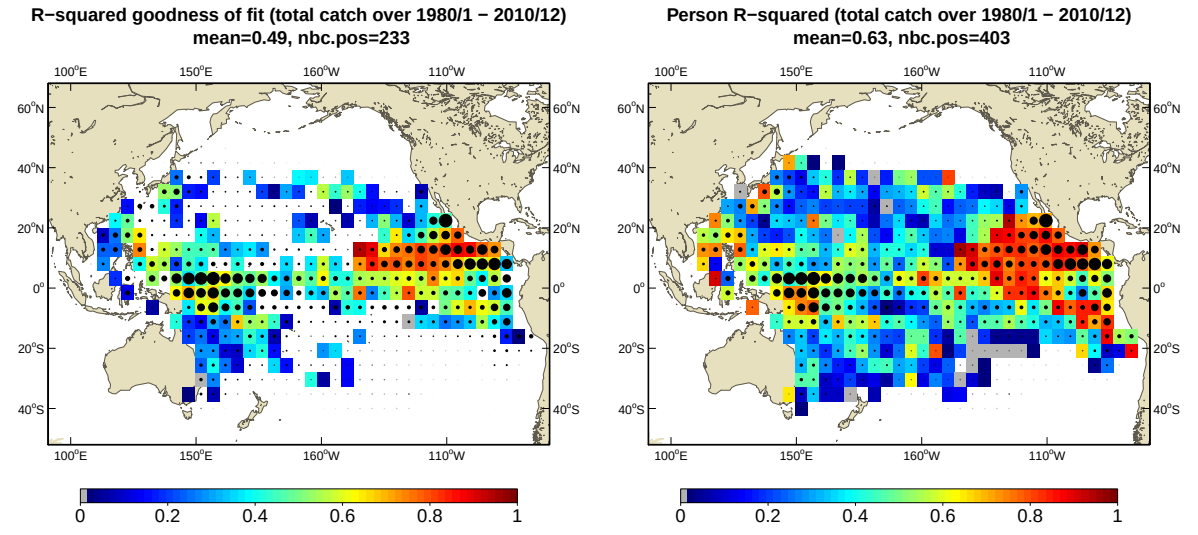

Figure 12: Spatial map of validation metrics: (left) R-squared goodness of fit and (right) squared Pearson correlation coefficient.

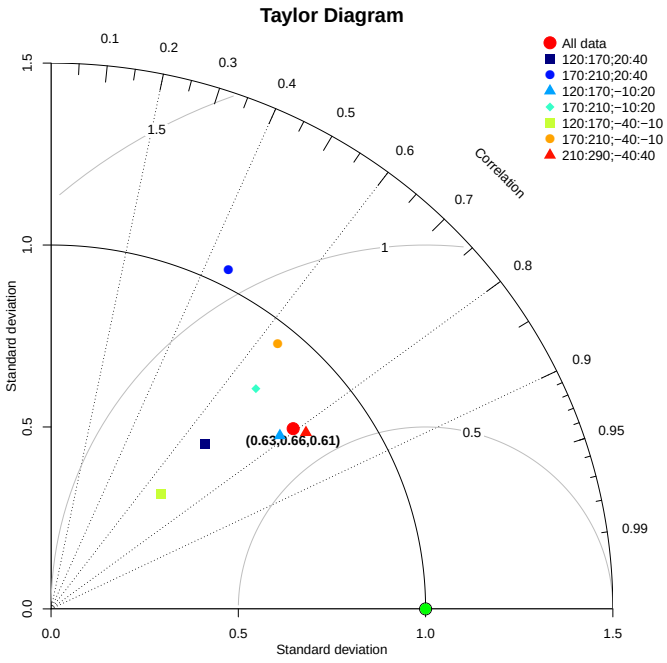

Figure 13: Taylor diagram, providing three aggregated metrics of model fit to the data: standard deviation (distance from (0,0) point depicts the ration between model and data standard deviation), correlation (angular coordinates) and normalized mean squared error (concentric circles with the green bullet being the center)

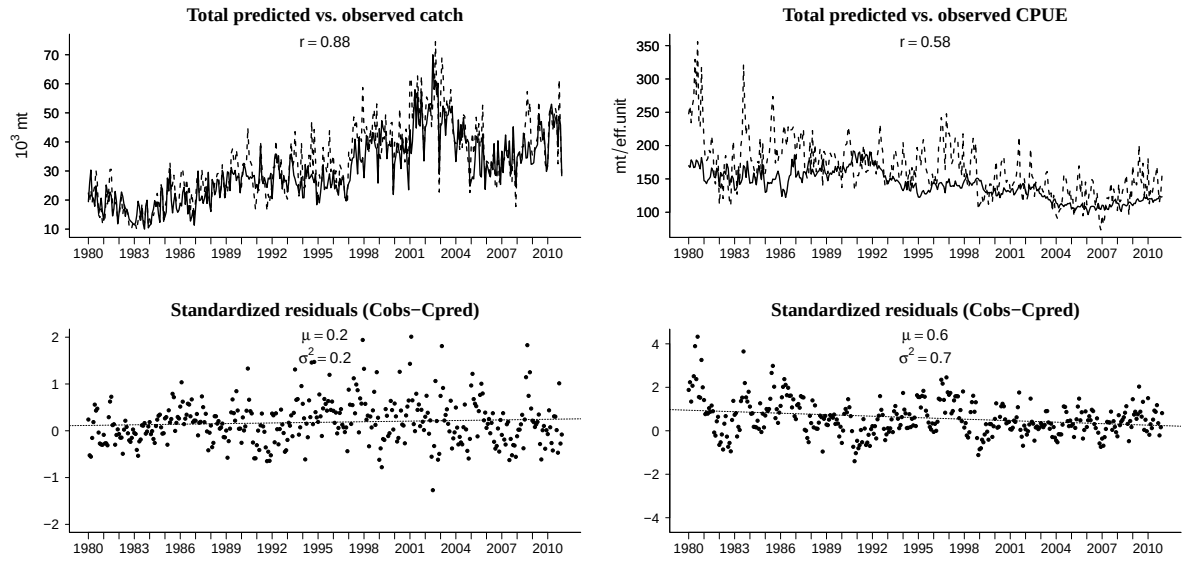

Figure 14: Monthly time series of total observed and predicted catch (left) and CPUE (right) with their standardized residuals

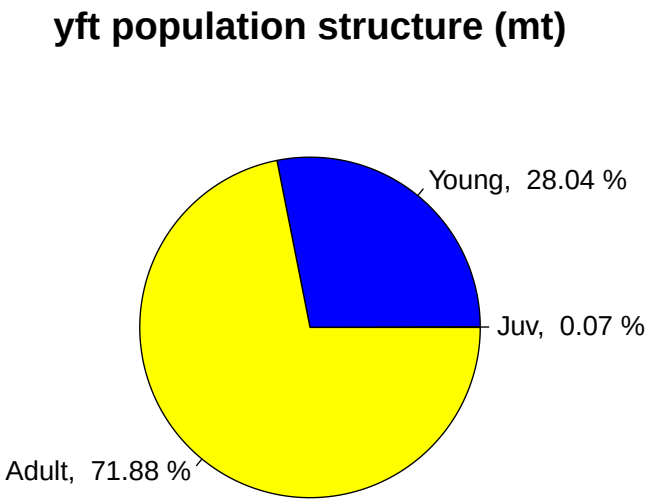

Figure 15: Population composition by life stage

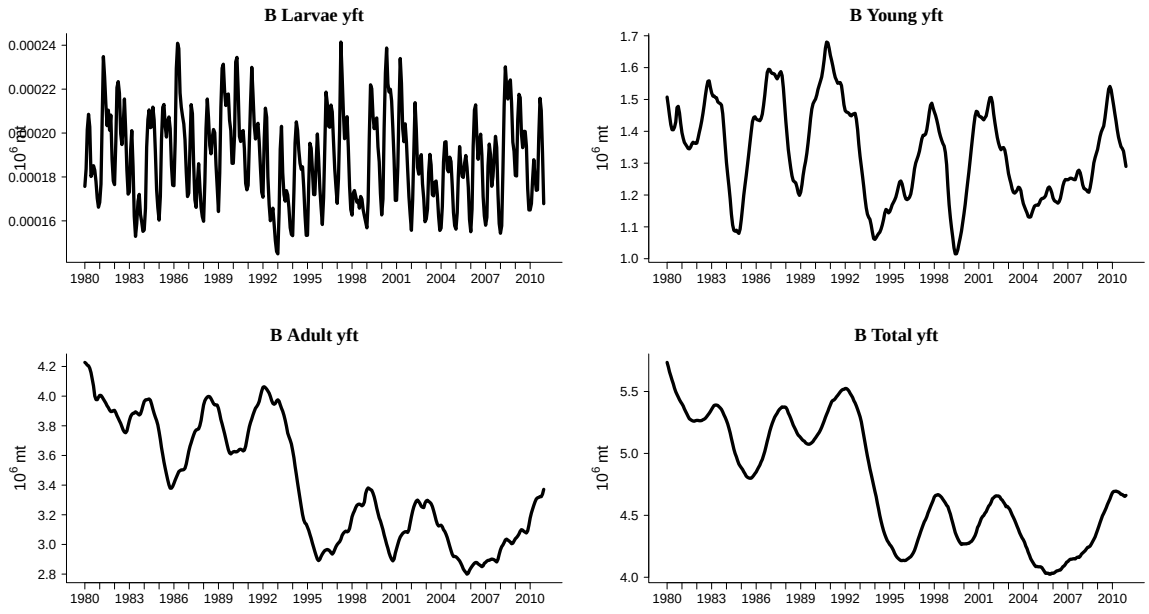

Figure 16: Time series of (from top to bottom) Larvae, young, adult and total biomass

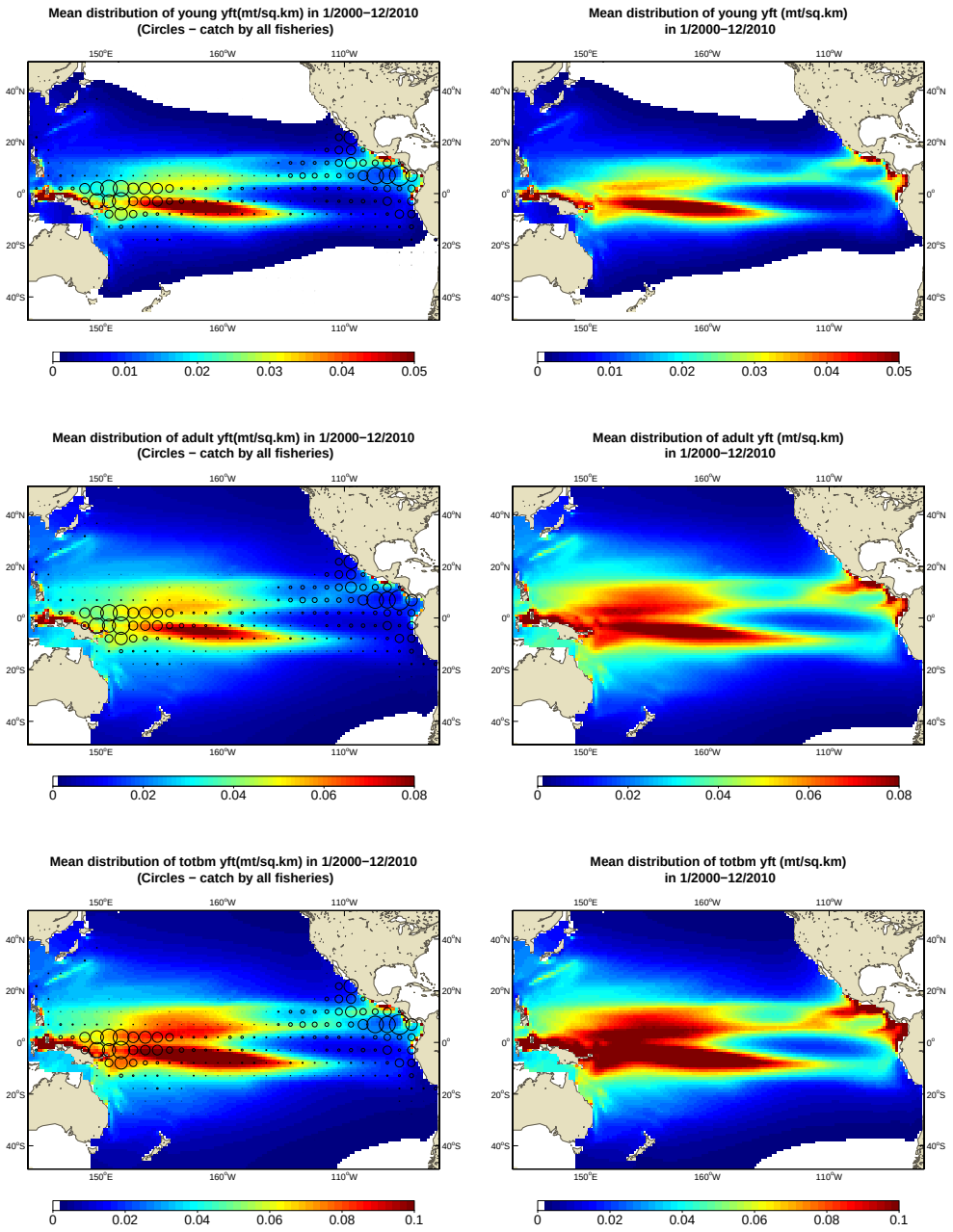

Figure 17: Average spatial distributions of (from top to bottom) young, adult and total biomass with (left) and without fishing (right)

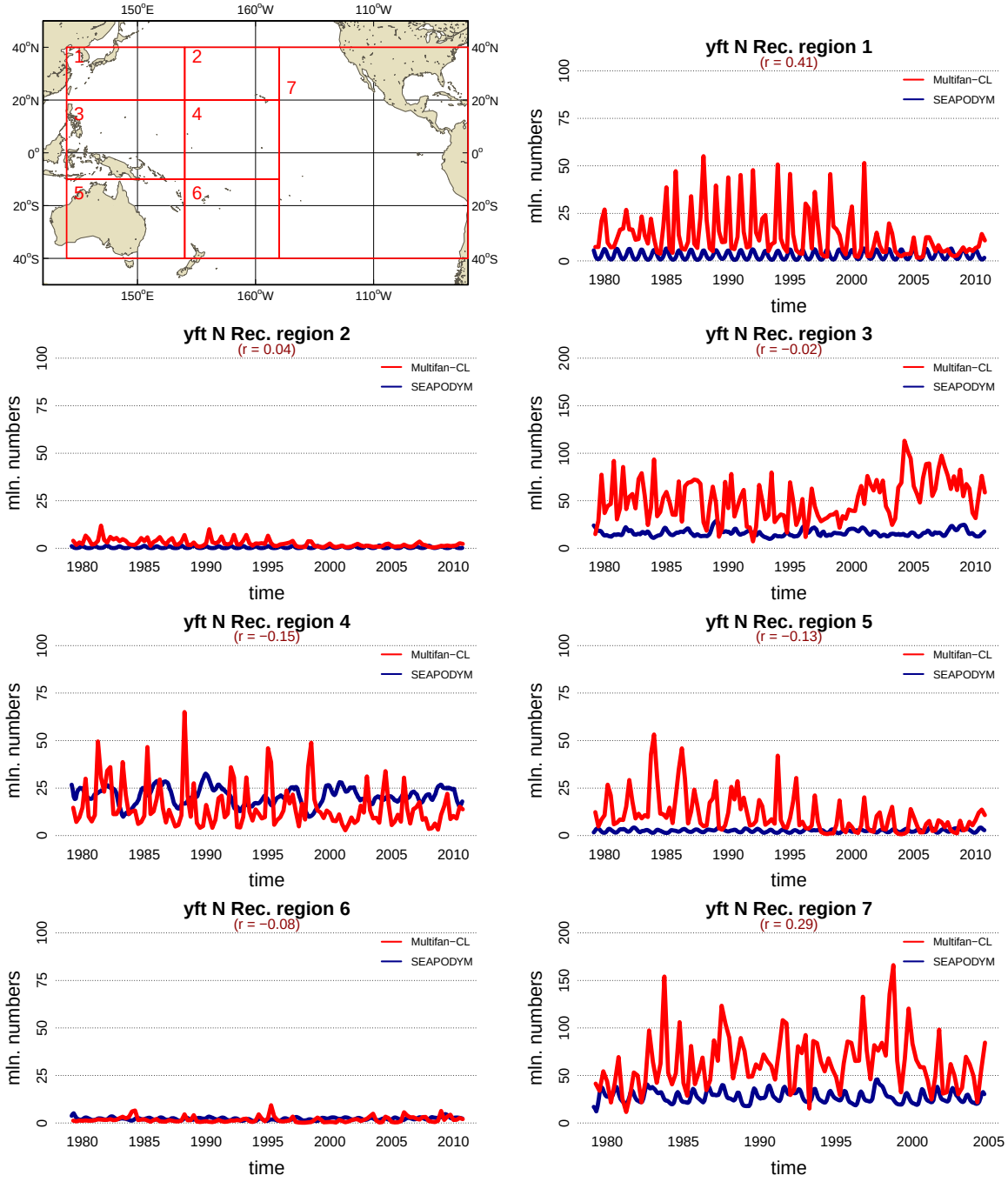

Figure 18: Regional comparison between SEAPODYM and Multifan-CL model predictions for recruitment

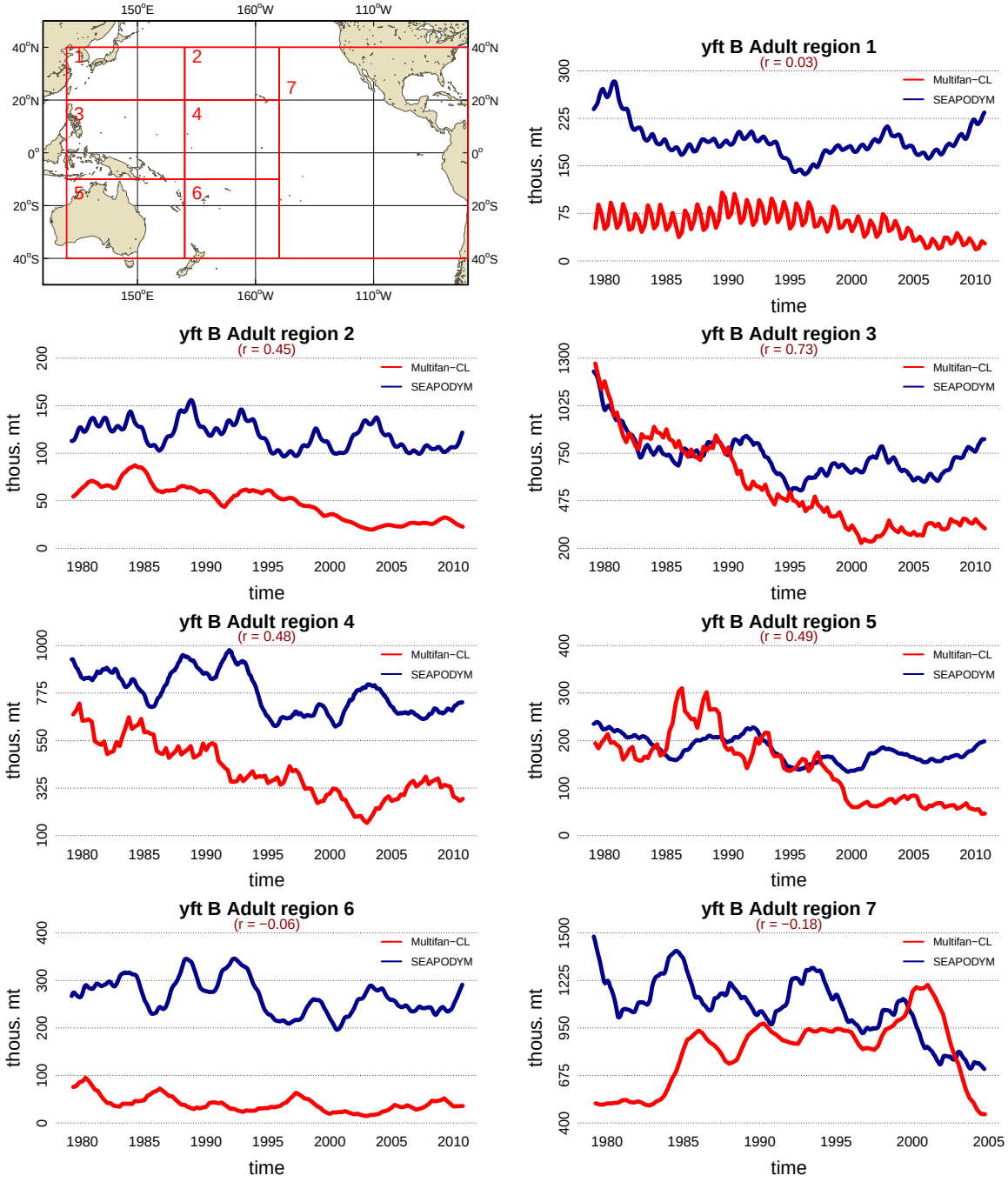

Figure 19: Regional comparison between SEAPODYM and Multifan-CL model predictions for spawning biomass

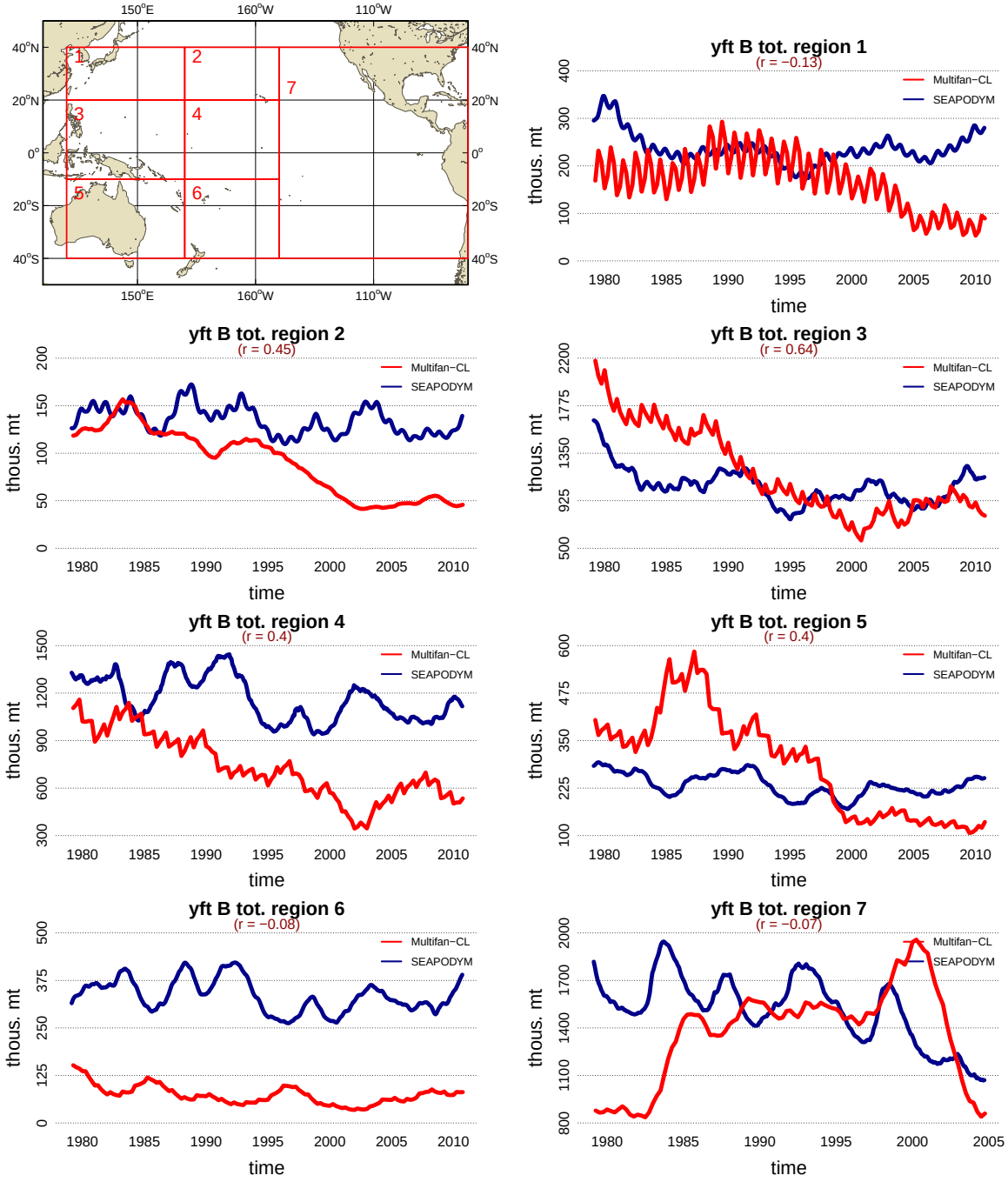

Figure 20: Regional comparison between SEAPODYM and Multifan-CL model predictions for total (immature and mature) biomass

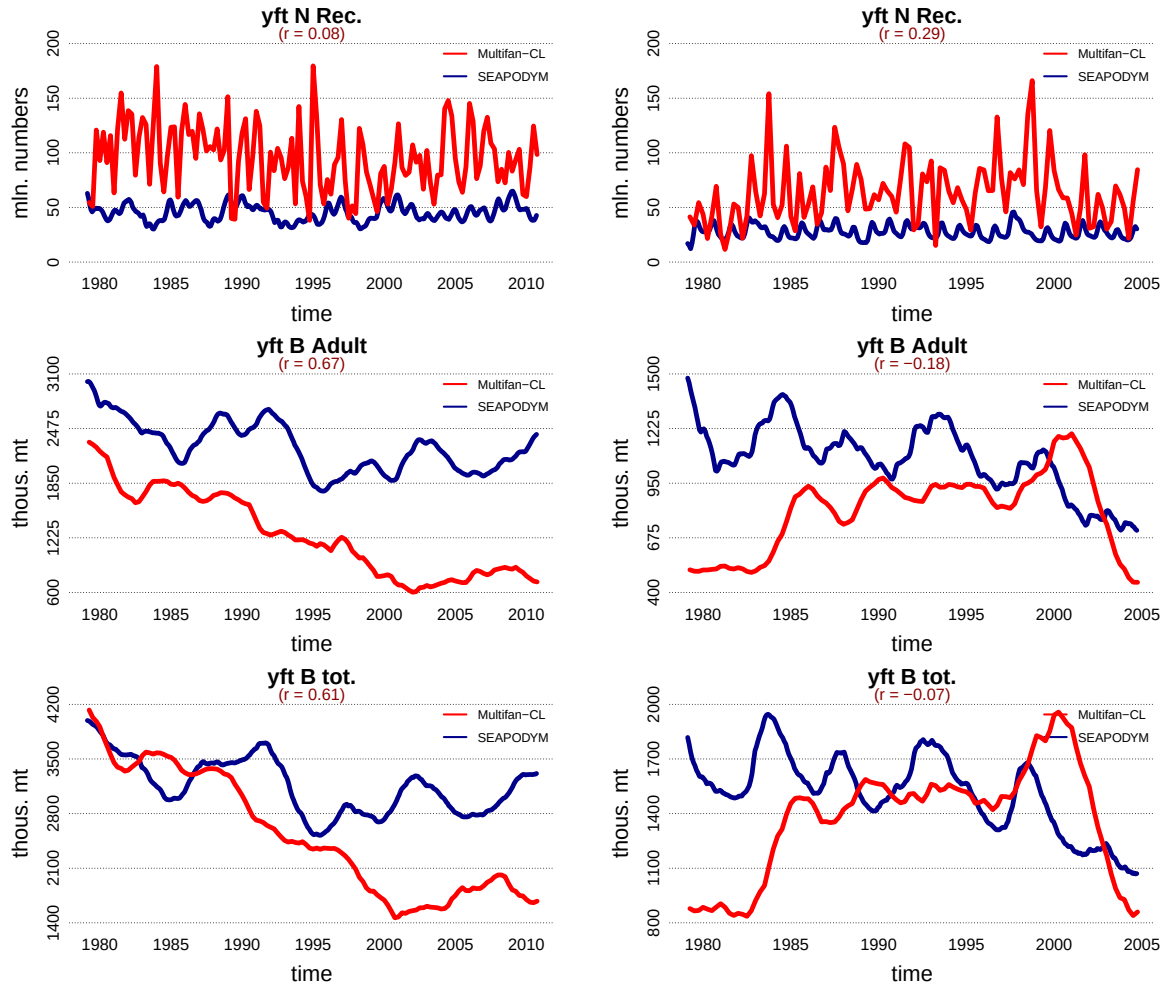

Figure 21: Comparison of (from top to bottom) recruitment, spawning and total biomass predicted by SEAPODYM and Multifan-CL models for WCPO (left) and EPO (right) (immature and mature) biomass

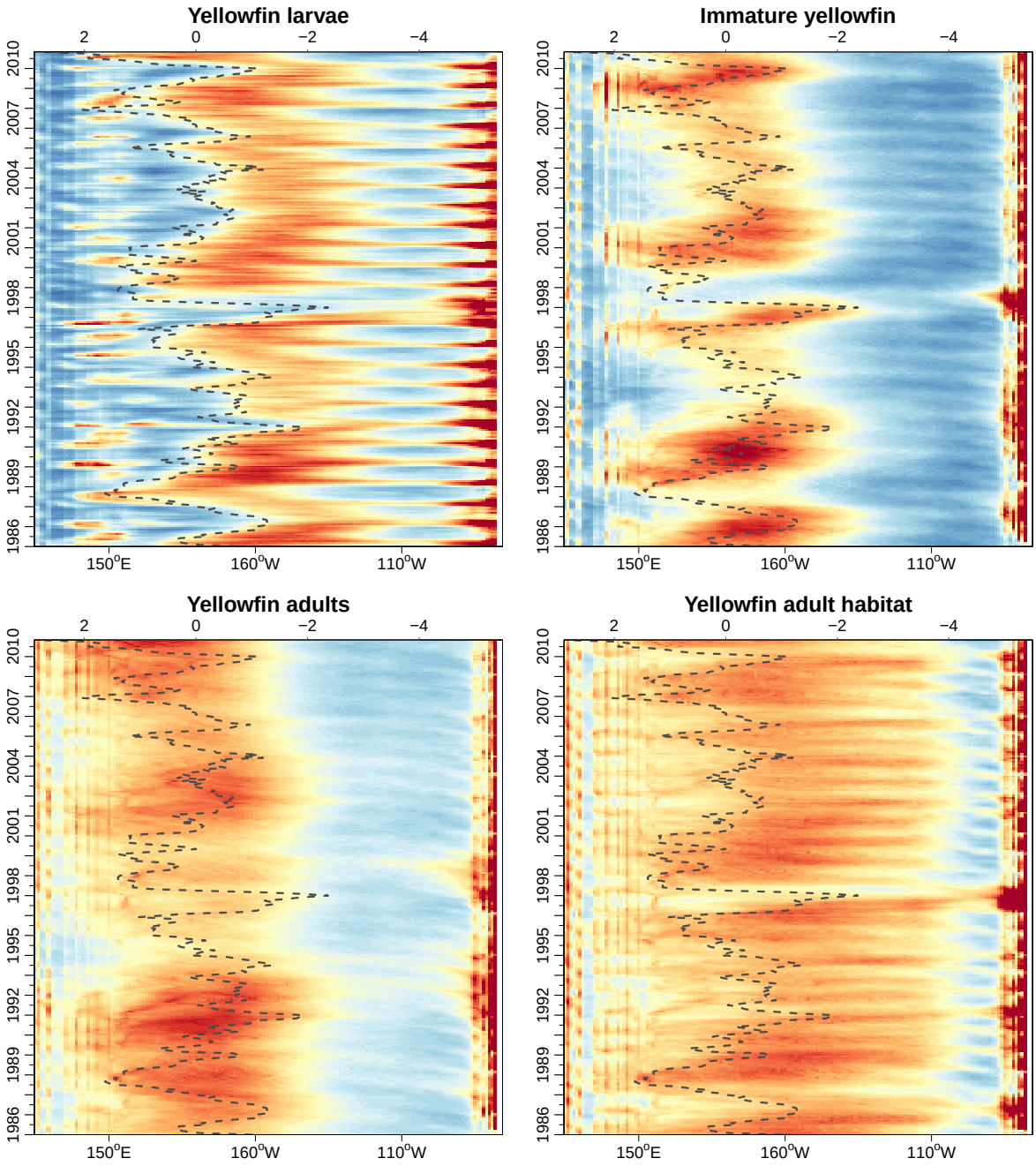

Figure 22: Variability of tropical (average over 10°S-10°N) biomass of larvae, and young and adult yellowfin and adult (3-yr old) habitat and Southern Oscillation Index (axis on the top of the map).

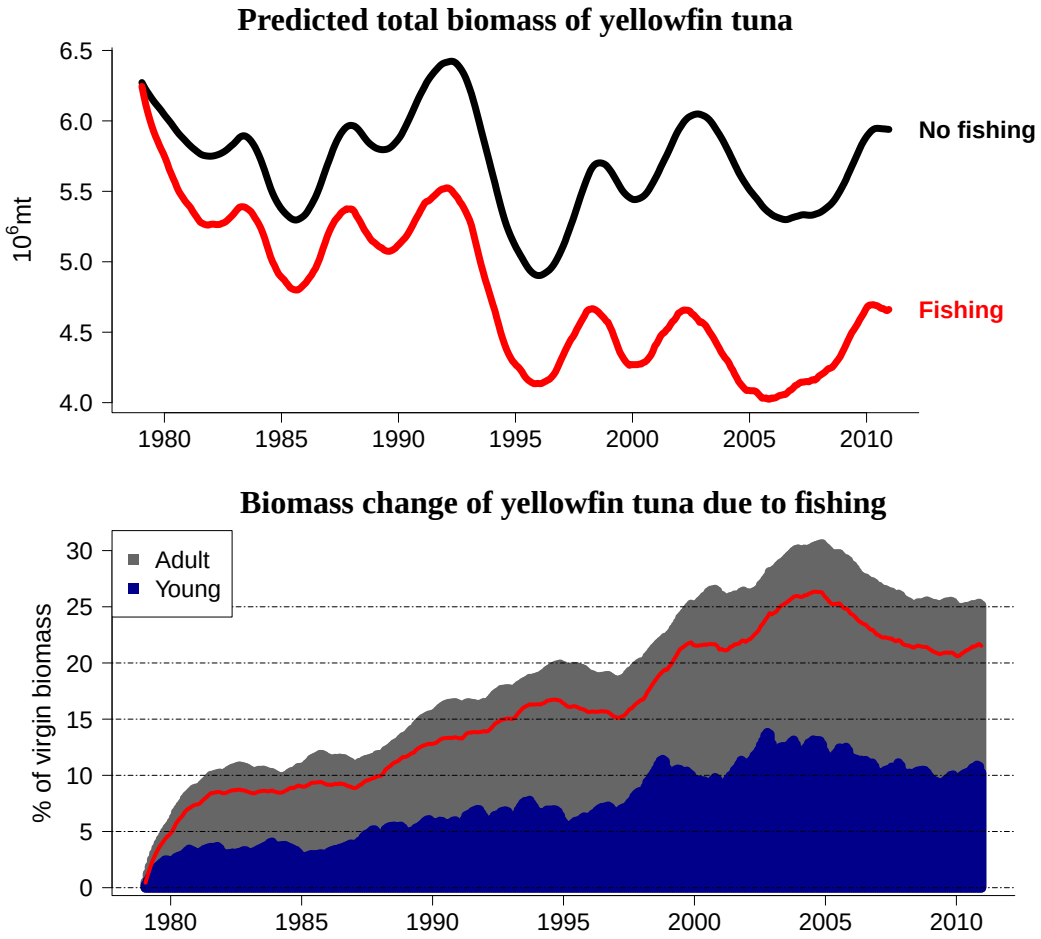

Figure 23: Quantification of fishing impact on young and adult population stages

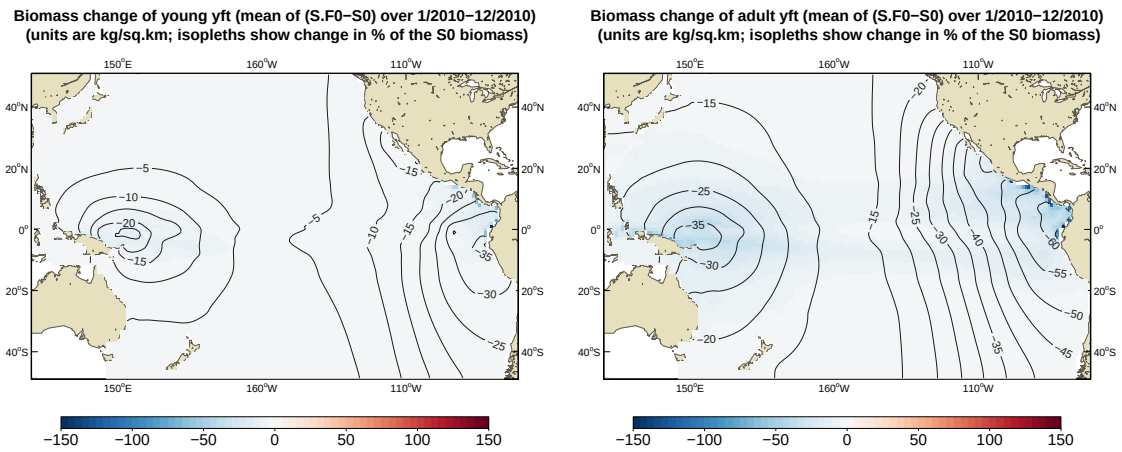

Figure 24: Spatial fishing impact on young and adult population stages. Contour lines show the index $\frac{B_{F0}-B_{ref}}{B_{F0}}$ and colour shows the average biomass reduction due to fishing.

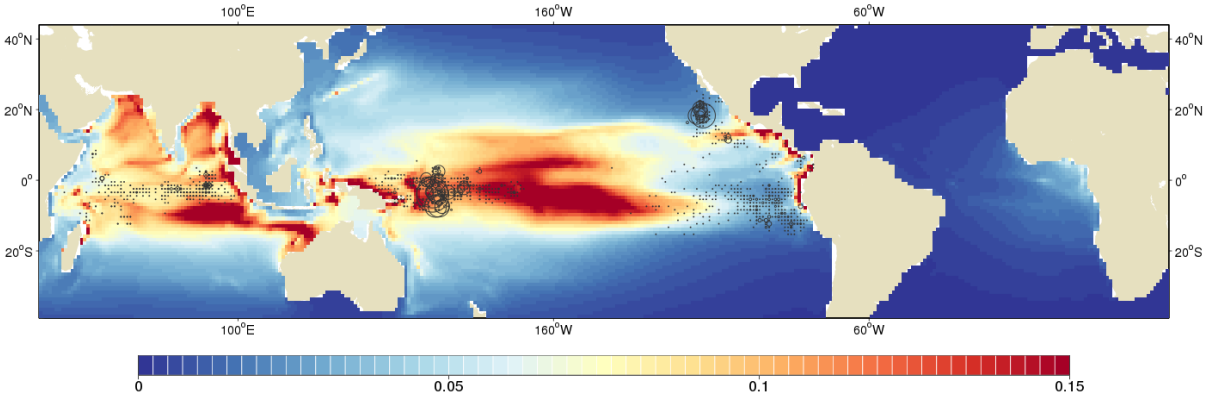

Figure 25: Snapshot of the total biomass of yellowfin tuna at the peak of El Niño episode in January 1998.

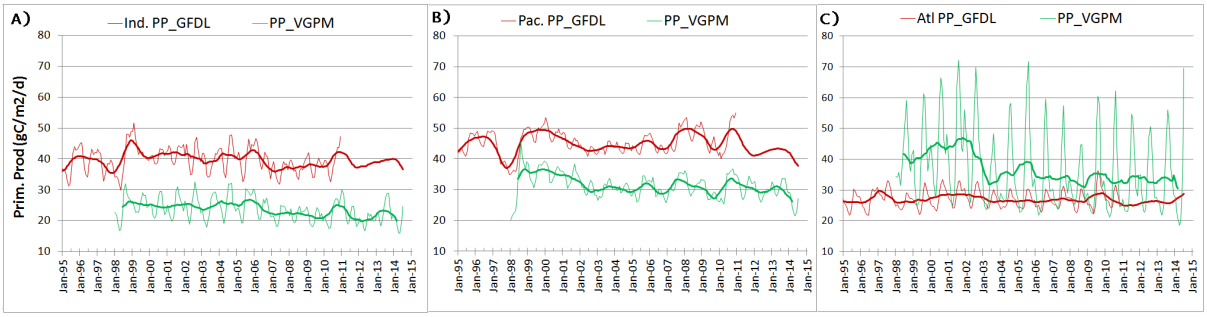

Figure 26: Comparison of primary production means predicted by INTERIM and estimated from satellite ocean color and VGPM model for three oceans.

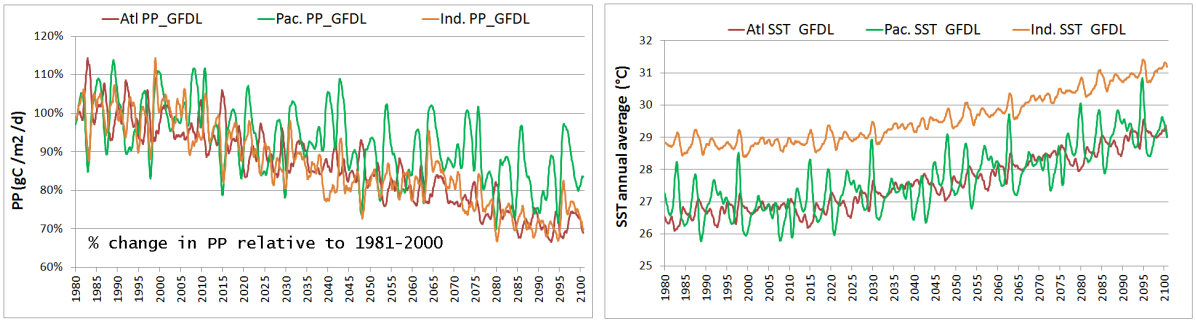

Figure 27: Percentage changes in Primary Production and SST variables predicted by INTERIM with NorESM, IPSL and GFDL forcing under IPCC RCP8.5 scenario.

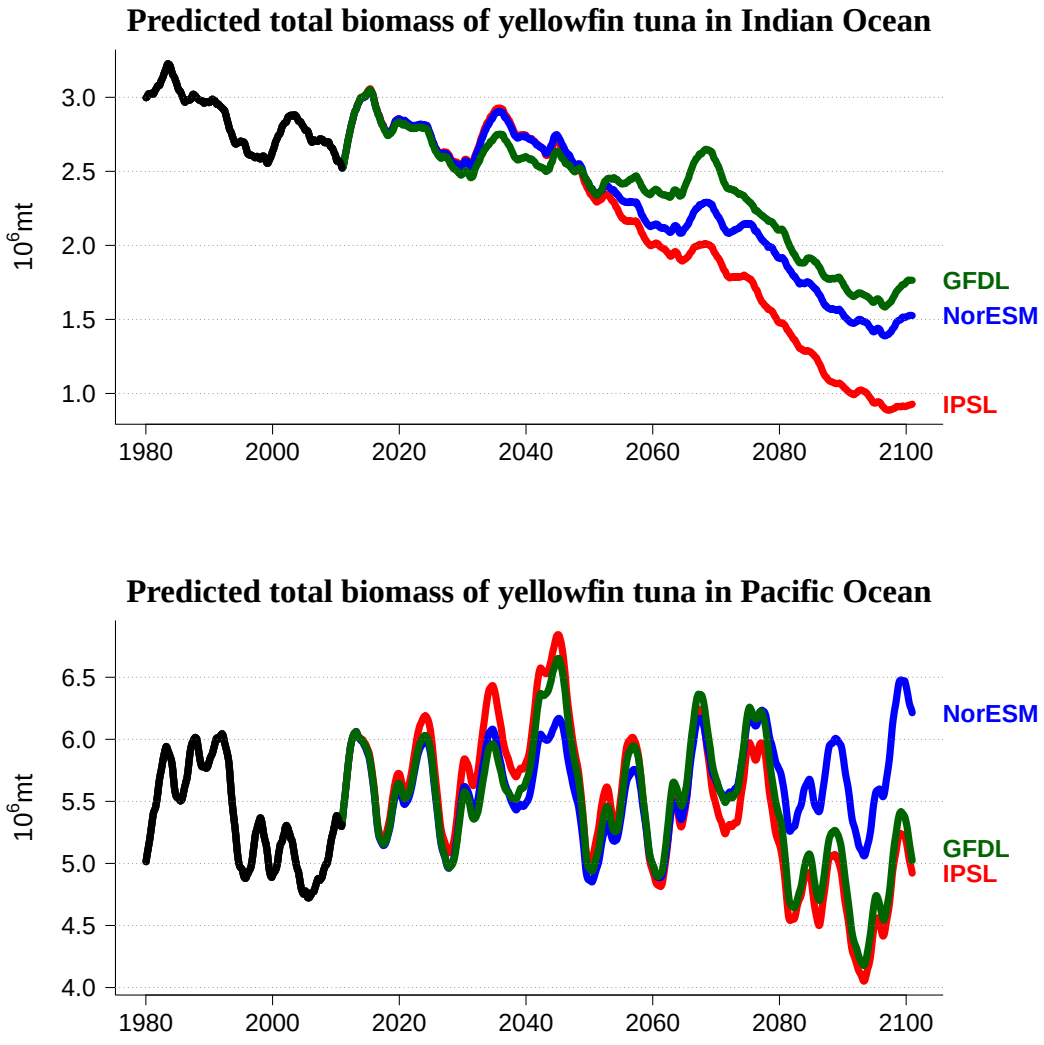

Figure 28: Predicted total biomass (historical simulation with fishing) and projected (without fishing) impact of climate change using atmospheric outputs from 3 different Earth Models under IPCC RCP8.5 scenario to drive the coupled physical-biogeochemical NEMO-PISCES model and then SEAPODYM.

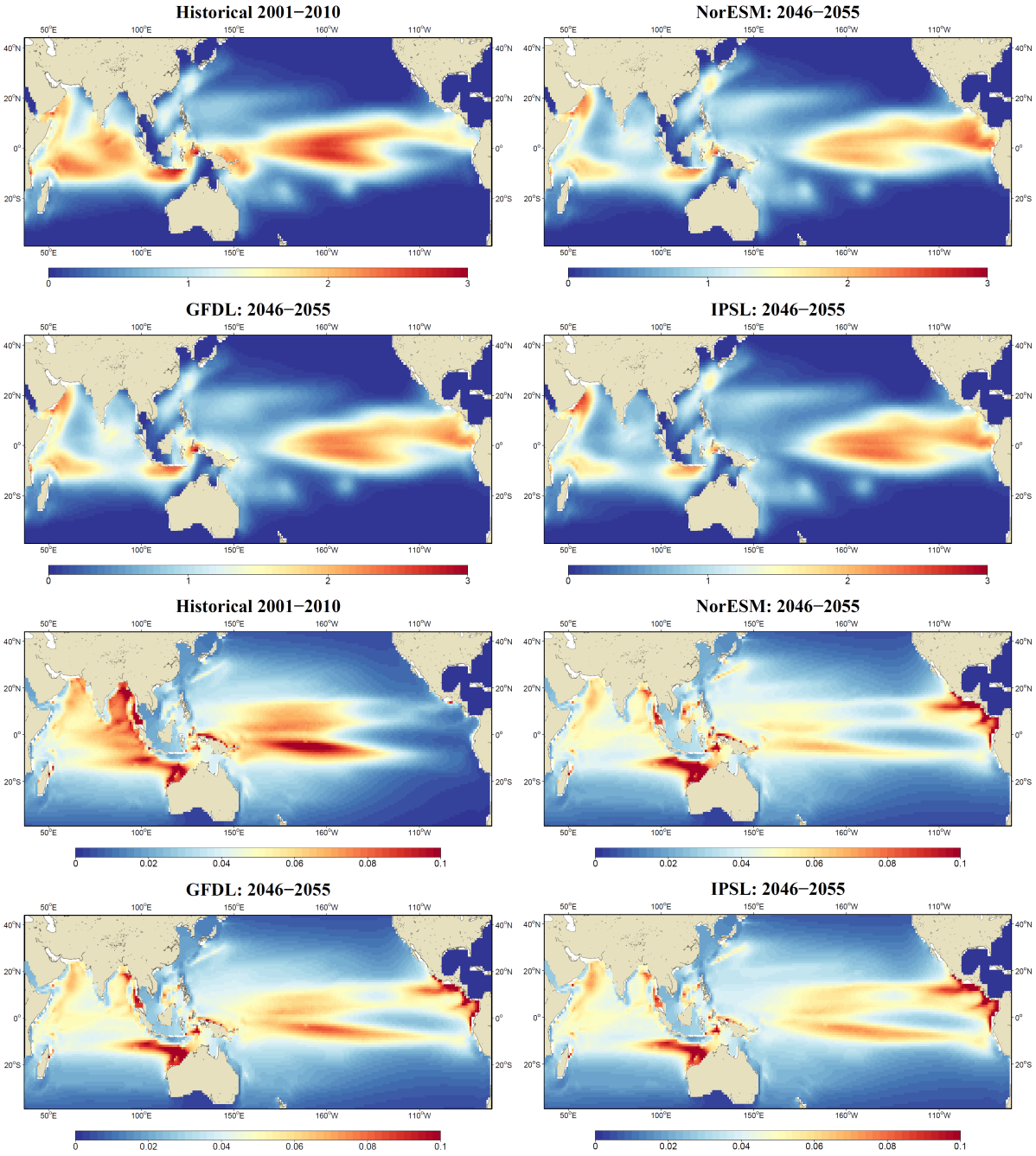

Figure 29: Larvae (top) in Nb/sq.km and adult (bottom) in mt/sq.km distributions of yellowfin tuna predicted with INTERIM historical (2001-2010) and 3 different future climate forcings from 3 Earth Models under IPCC RCP8.5 scenario.

A Appendices

A.1 Seapodym fisheries

A.2 Fit to the catch and LF data

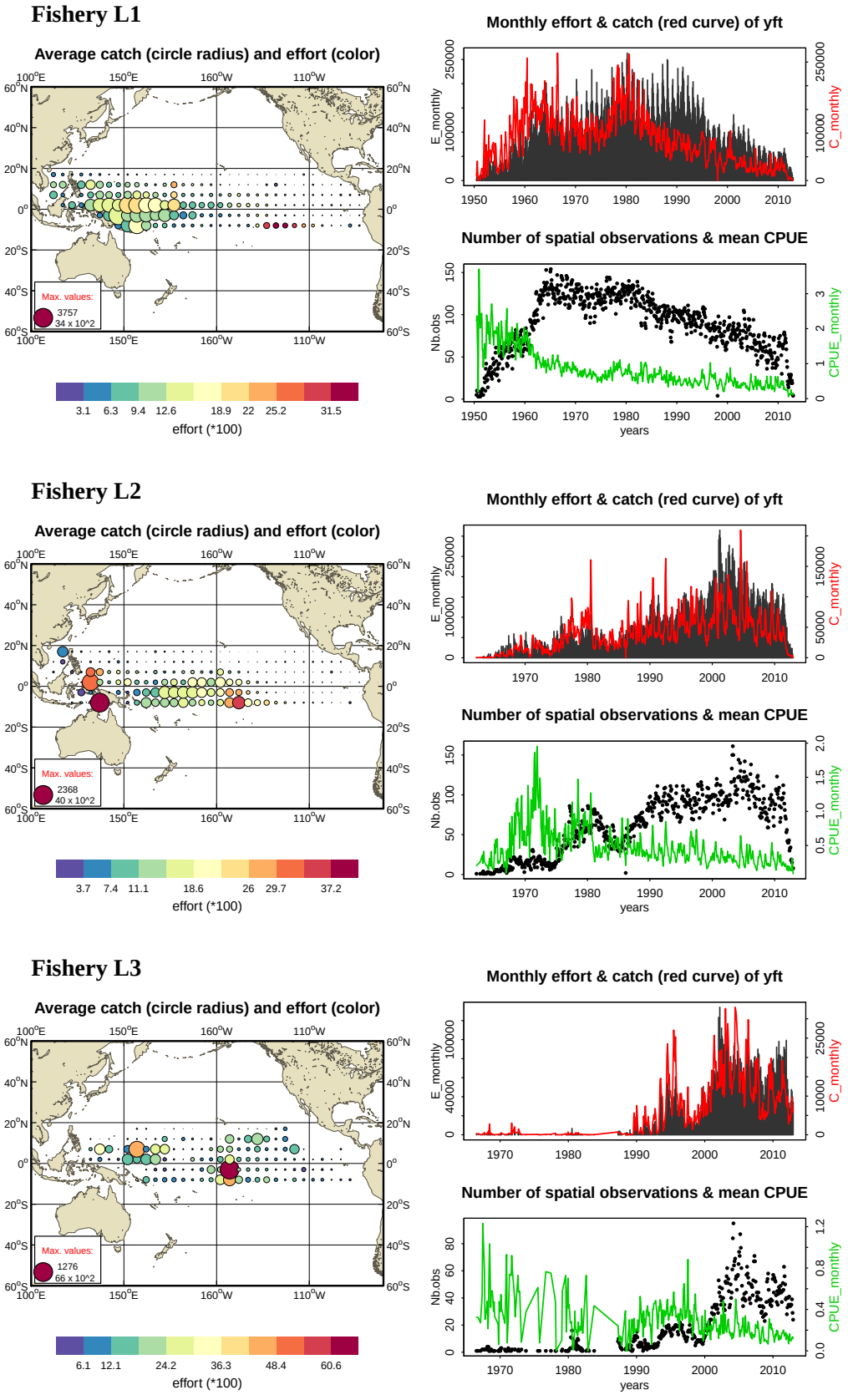

Figure 30: Spatial fishing dataset (effort and catch) being used in current SEAPODYM configuration

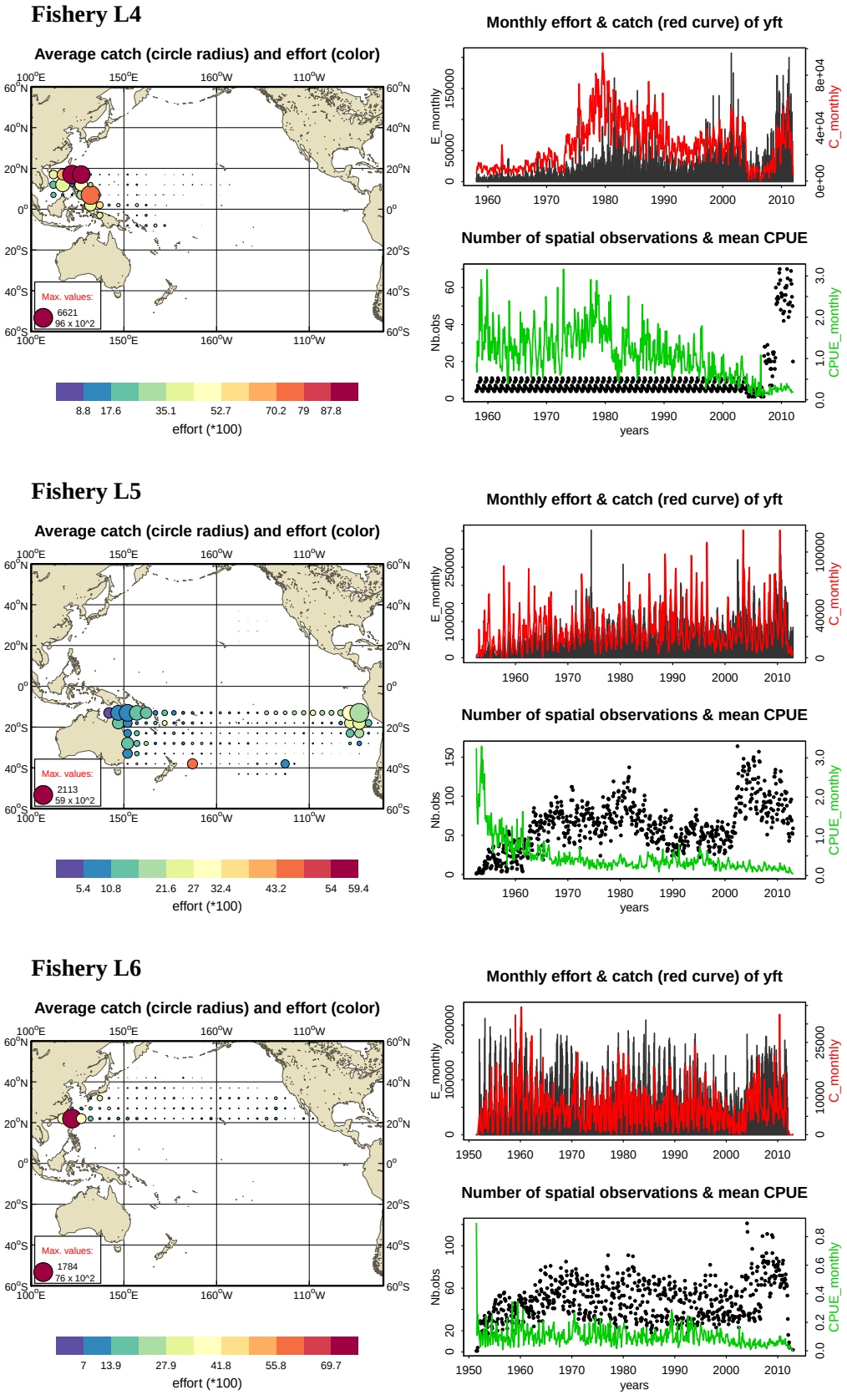

Figure 30: Spatial fishing dataset (effort and catch) being used in current SEAPODYM configuration (Continued)

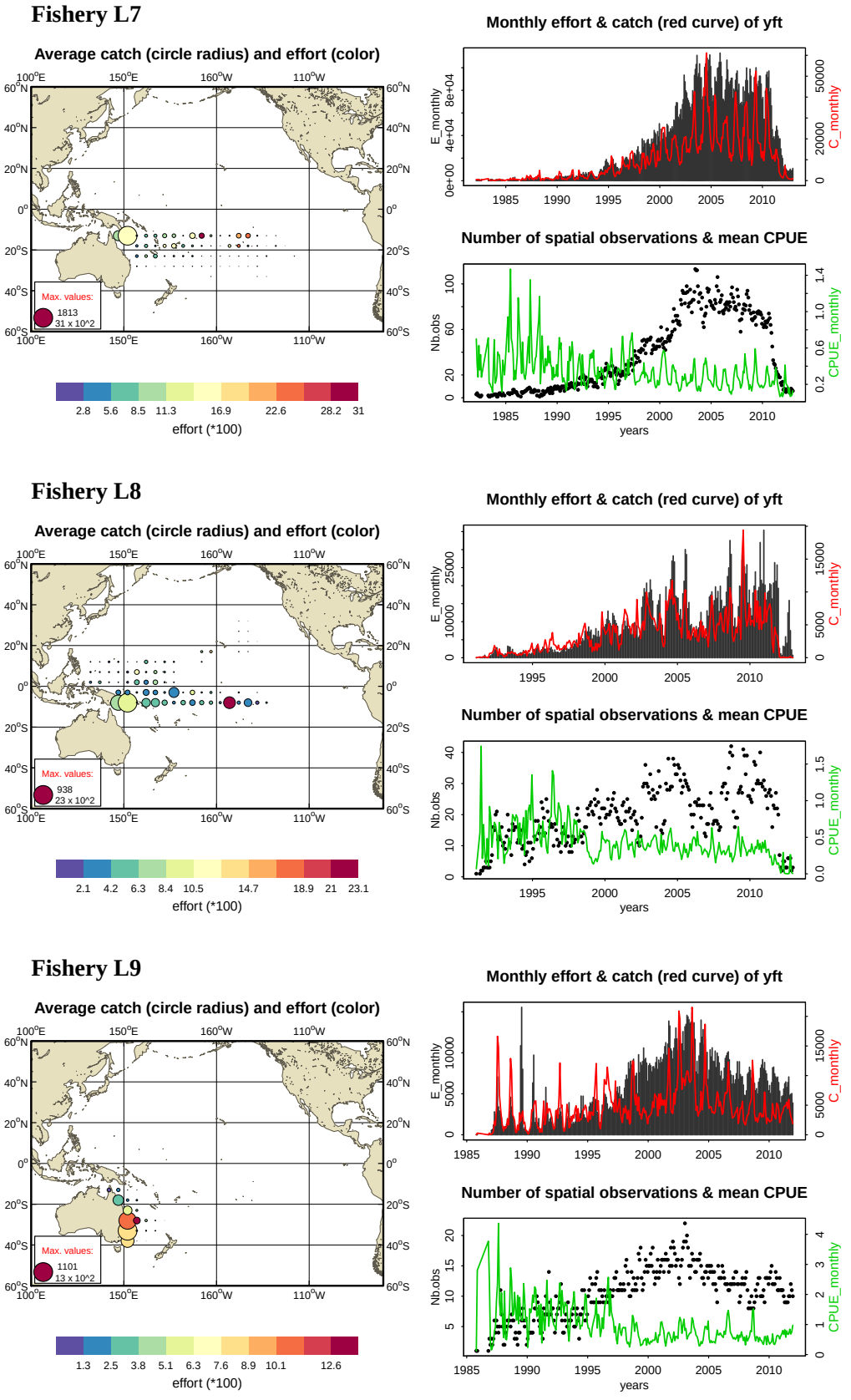

Figure 30: Spatial fishing dataset (effort and catch) being used in current SEAPODYM configuration (Continued)

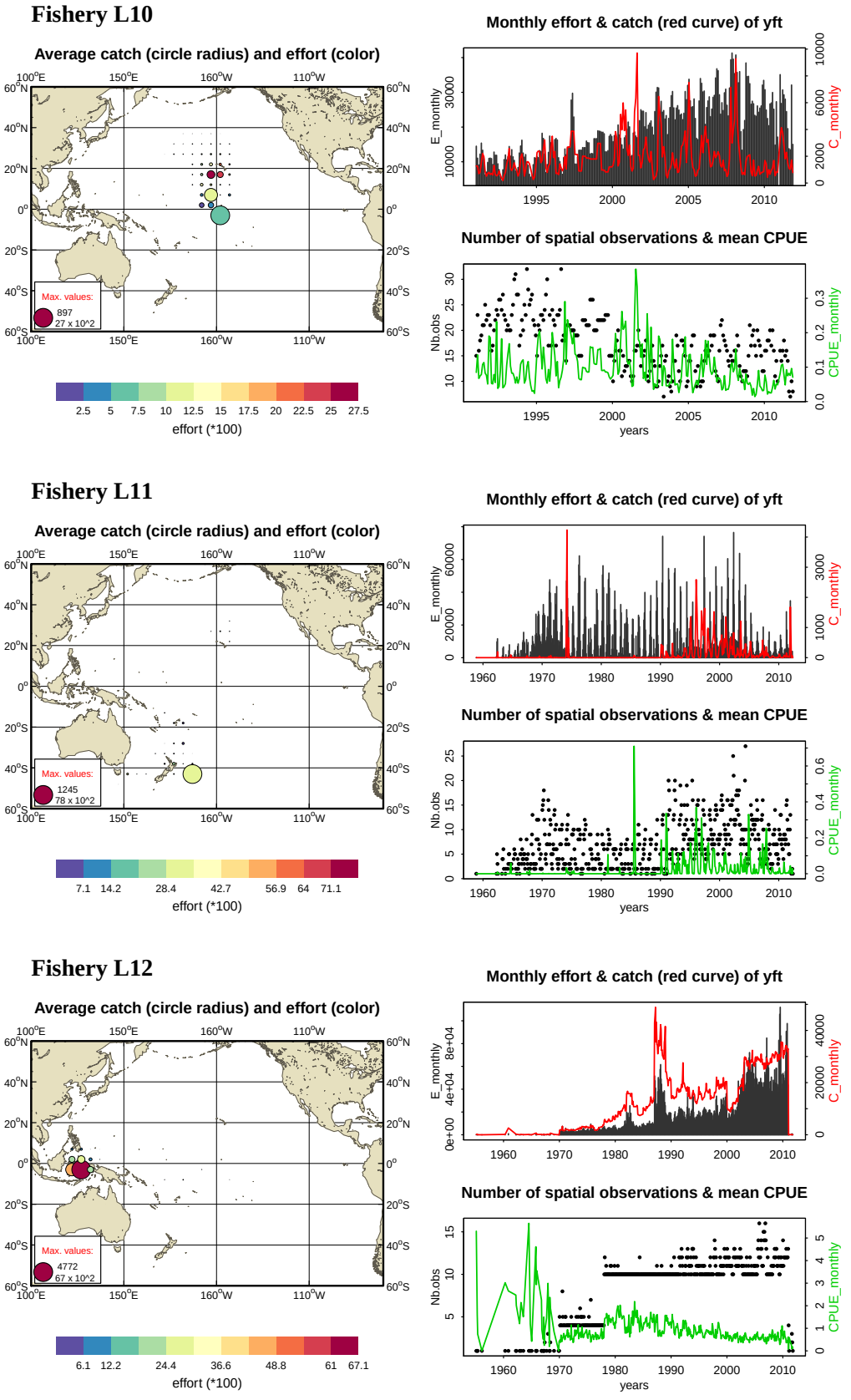

Figure 30: Spatial fishing dataset (effort and catch) being used in current SEAPODYM configuration (Continued)

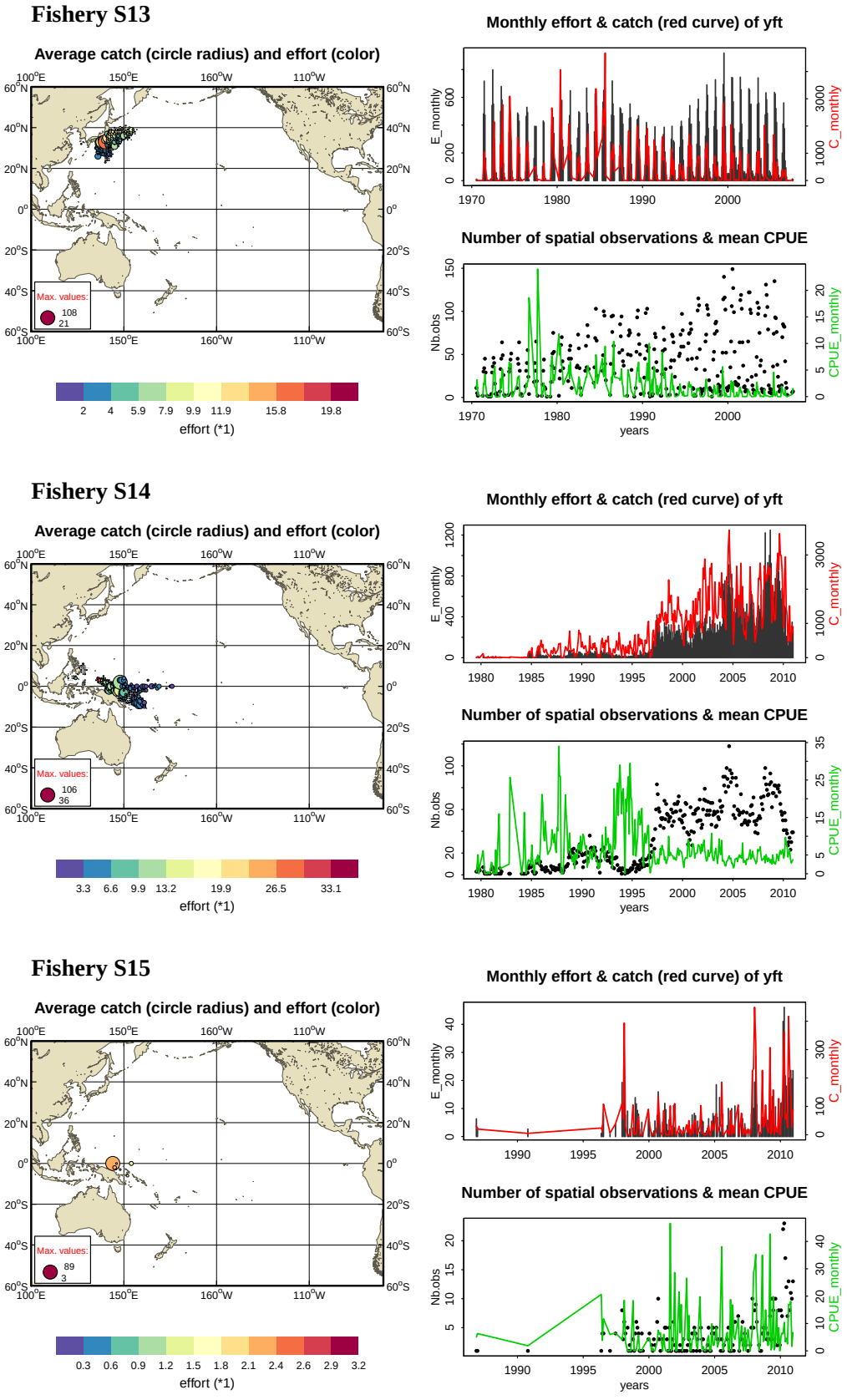

Figure 30: Spatial fishing dataset (effort and catch) being used in current SEAPODYM configuration (Continued)

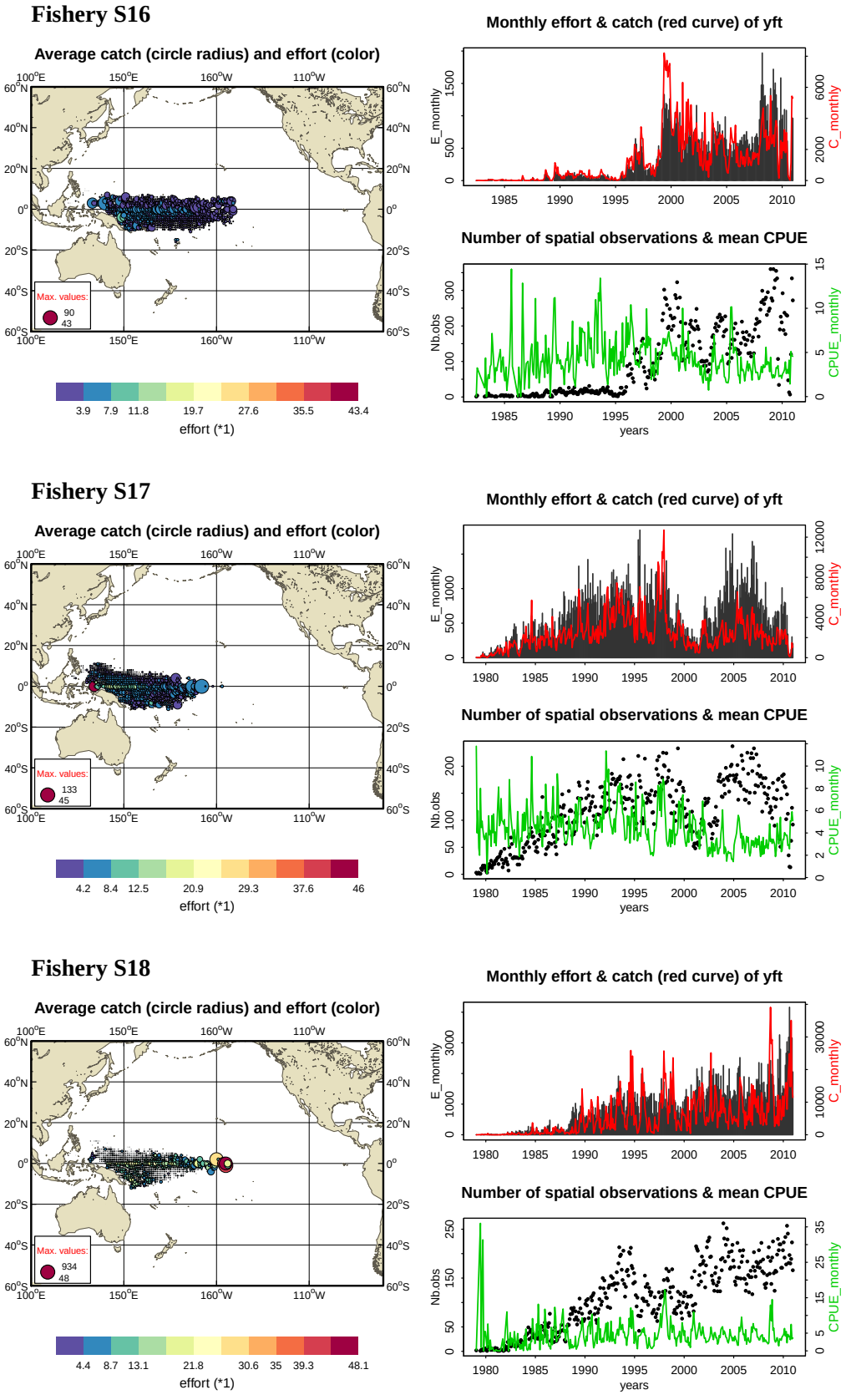

Figure 30: Spatial fishing dataset (effort and catch) being used in current SEAPODYM configuration (Continued)

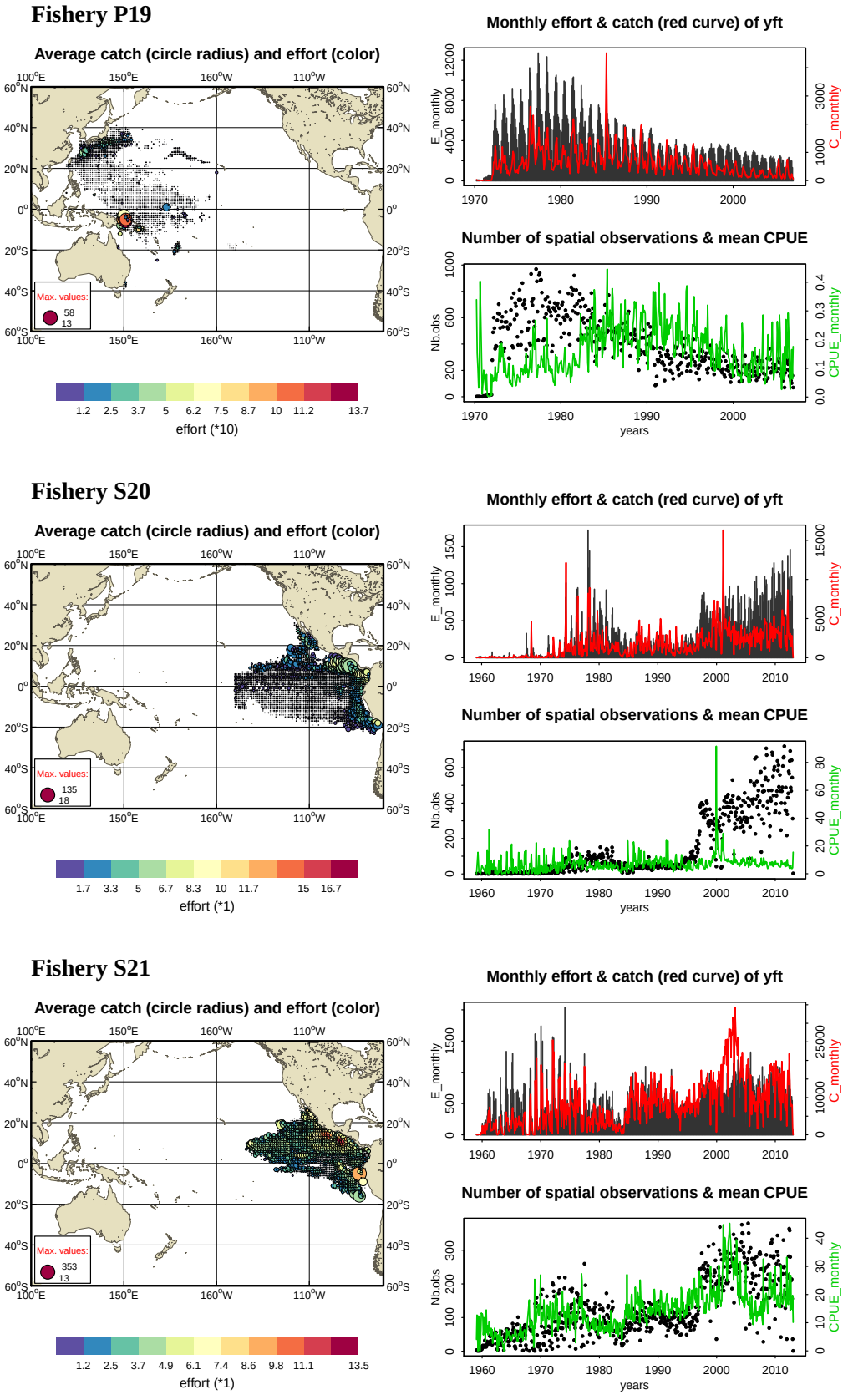

Figure 30: Spatial fishing dataset (effort and catch) being used in current SEAPODYM configuration (Continued)

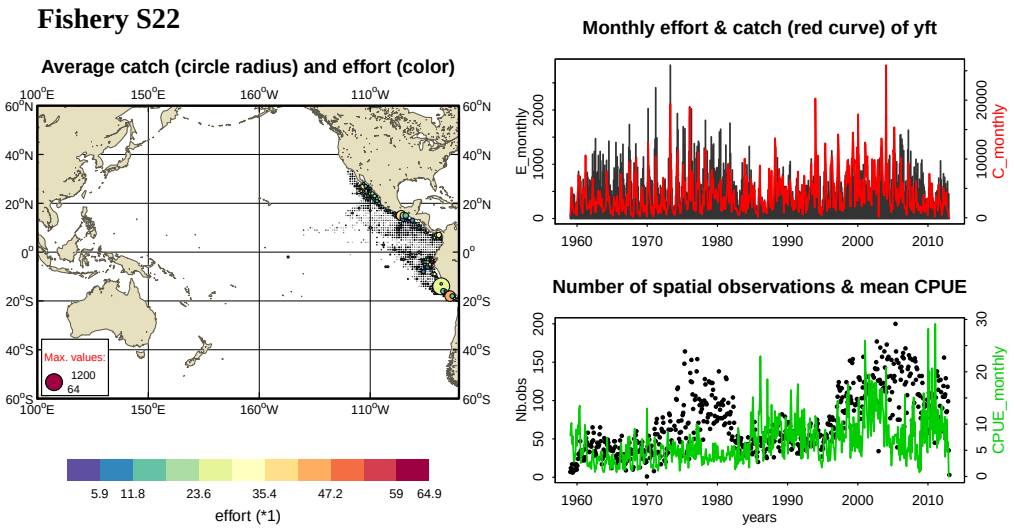

Figure 30: Spatial fishing dataset (effort and catch) being used in current SEAPODYM configuration (Continued)

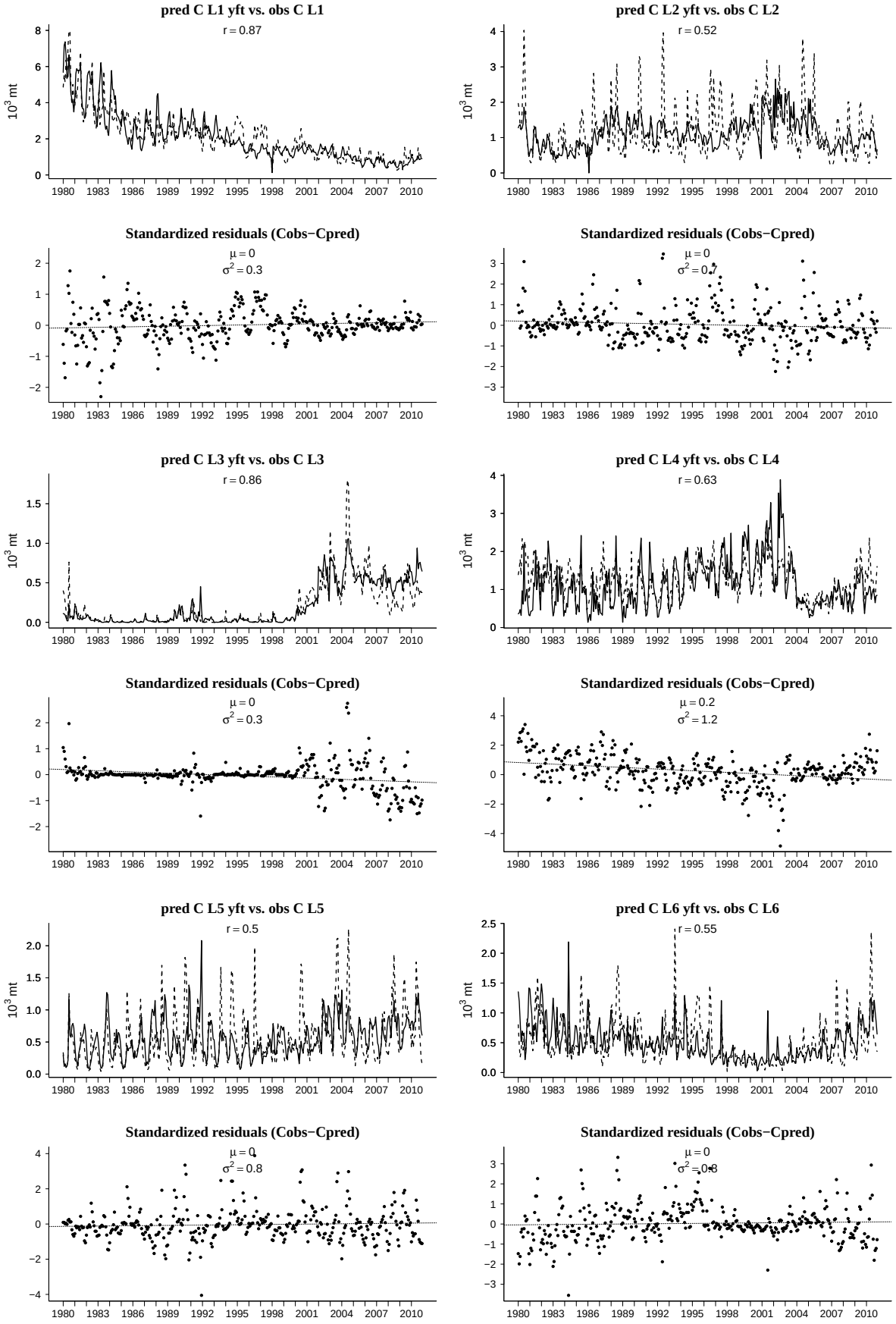

Figure 31: Monthly time series of observed and predicted catch by fishery

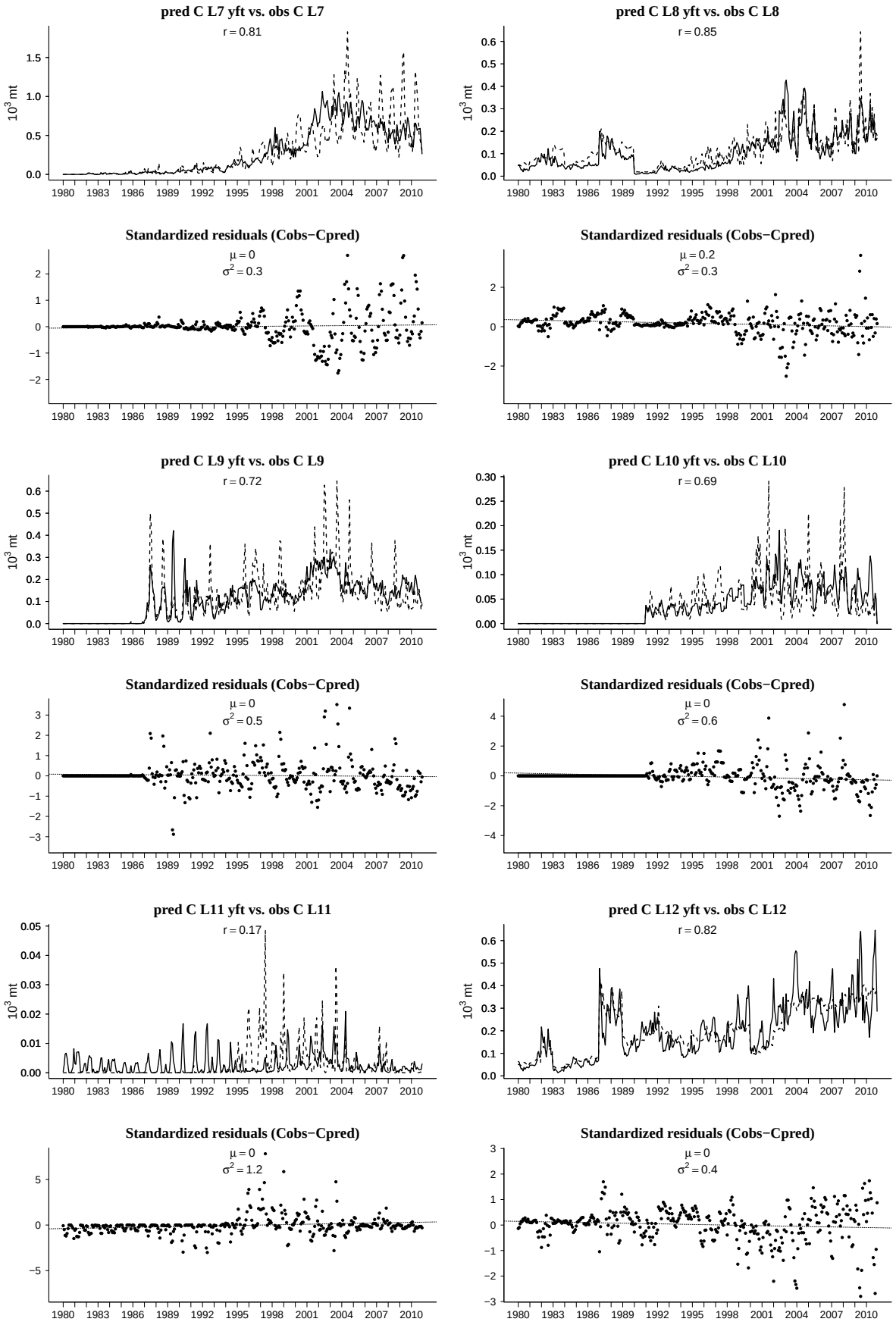

Figure 31: Monthly time series of observed and predicted catch by fishery (Continued)

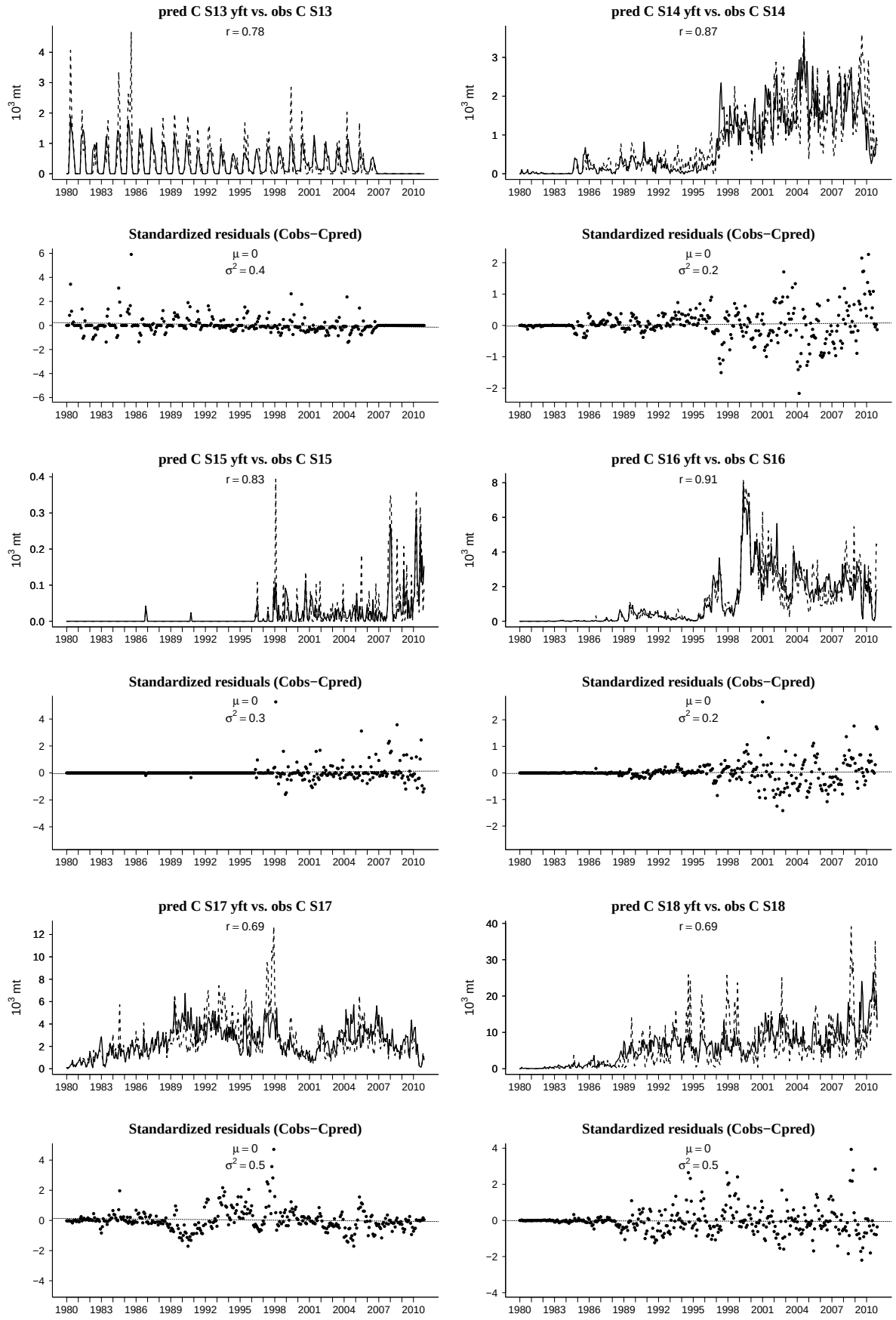

Figure 31: Monthly time series of observed and predicted catch by fishery (Continued)

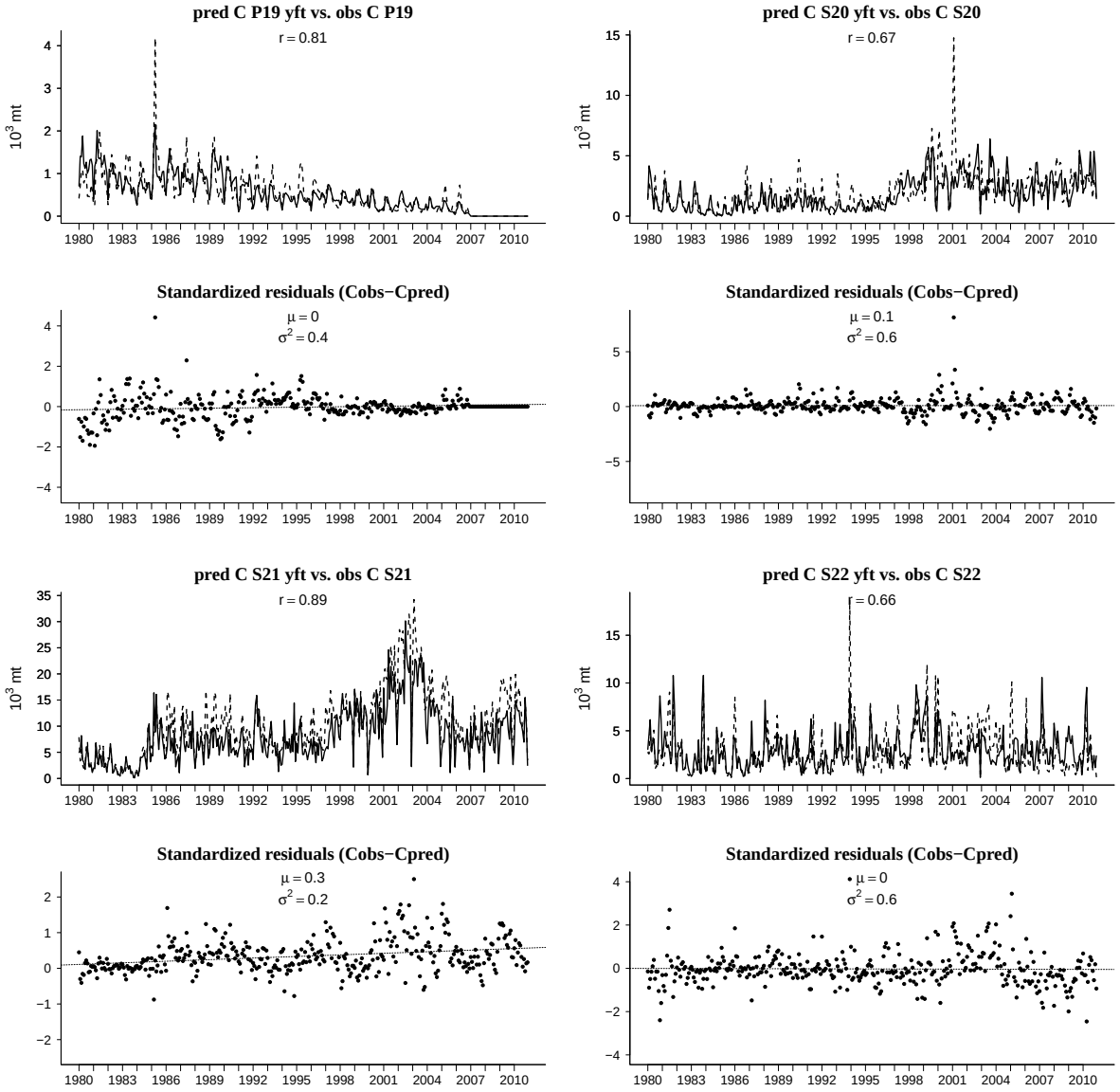

Figure 31: Monthly time series of observed and predicted catch by fishery (Continued)

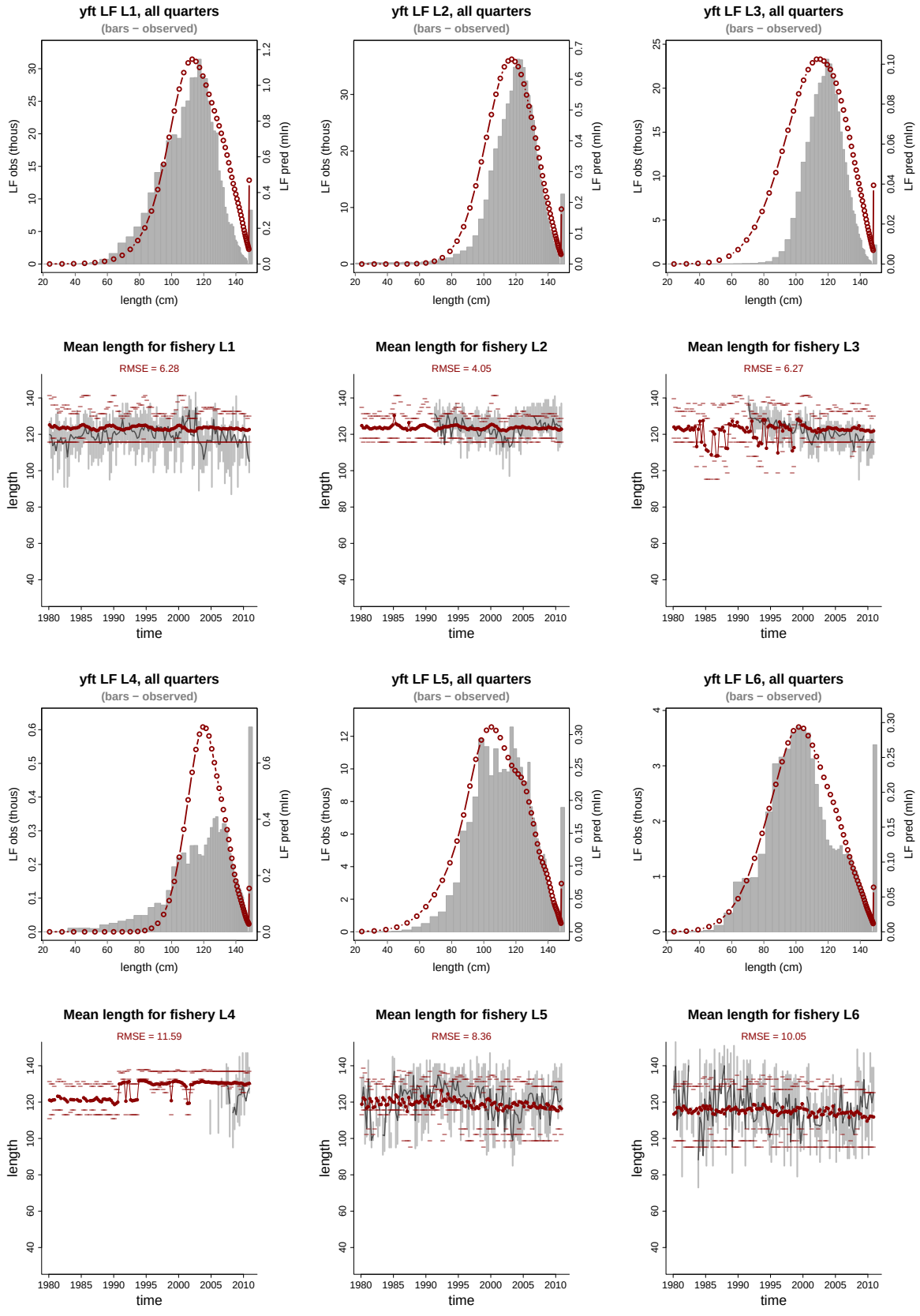

Figure 32: Observed (grey) and predicted (red) length frequencies distribution and mean length in catches.

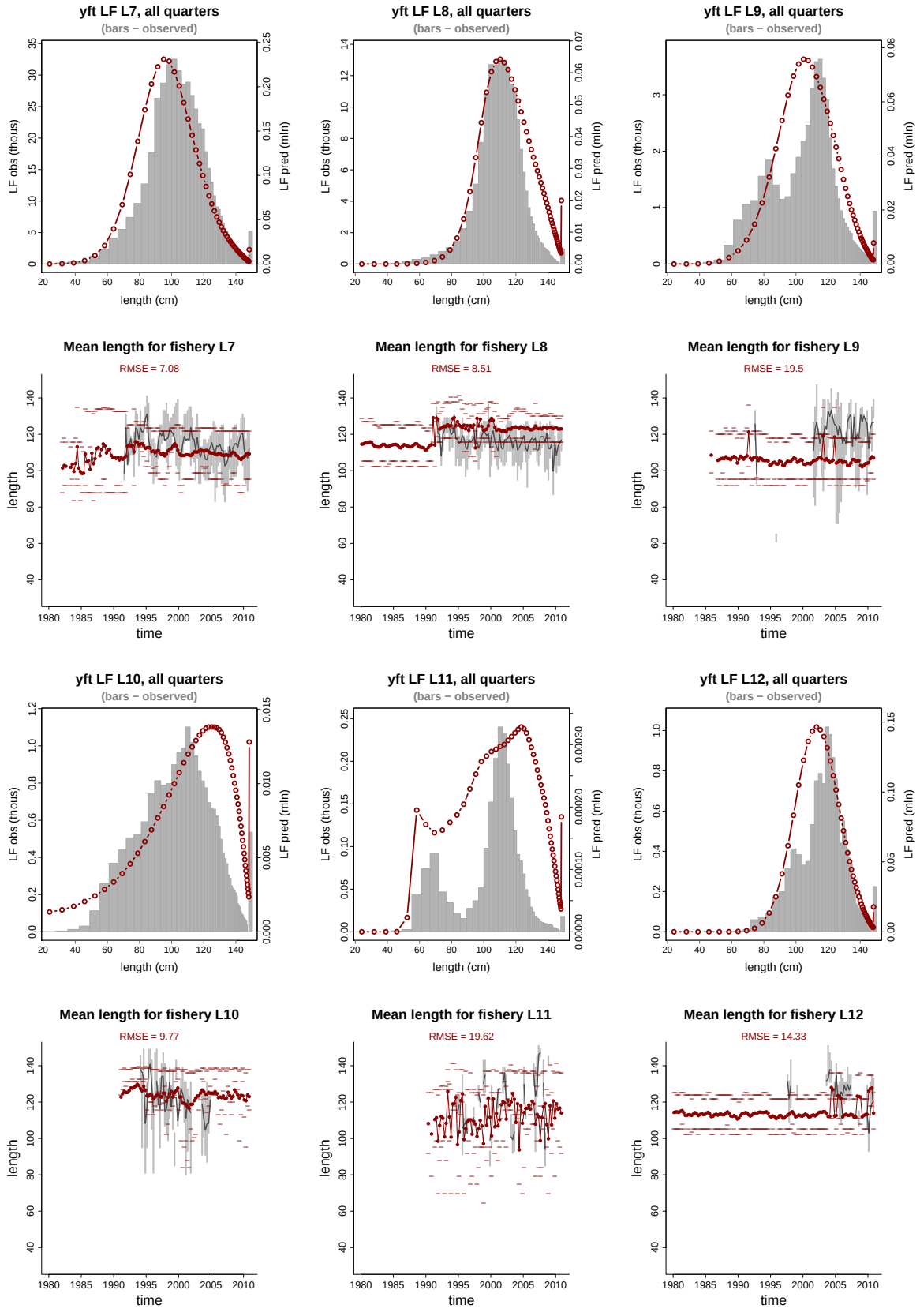

Figure 32: Continued

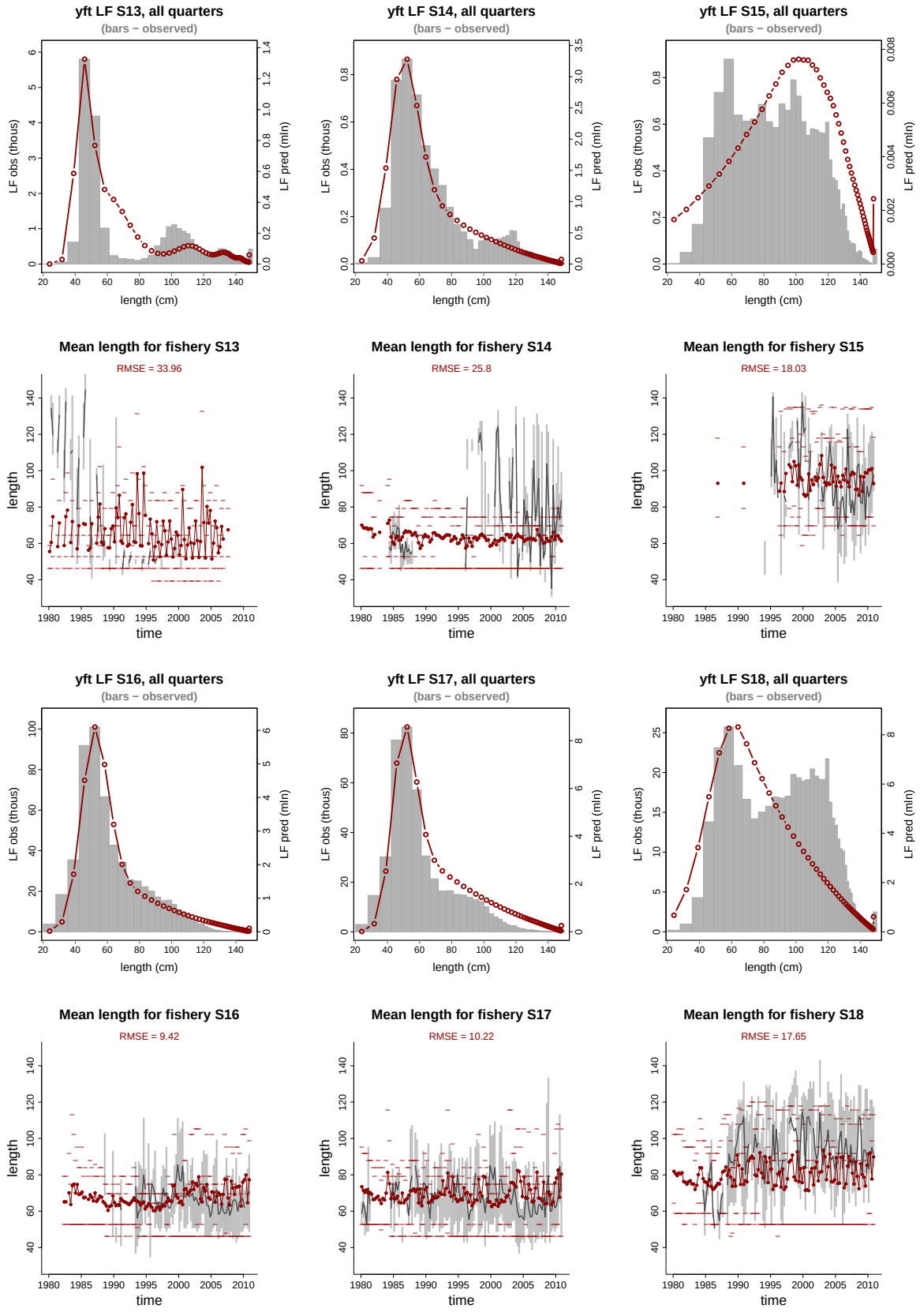

Figure 32: Continued

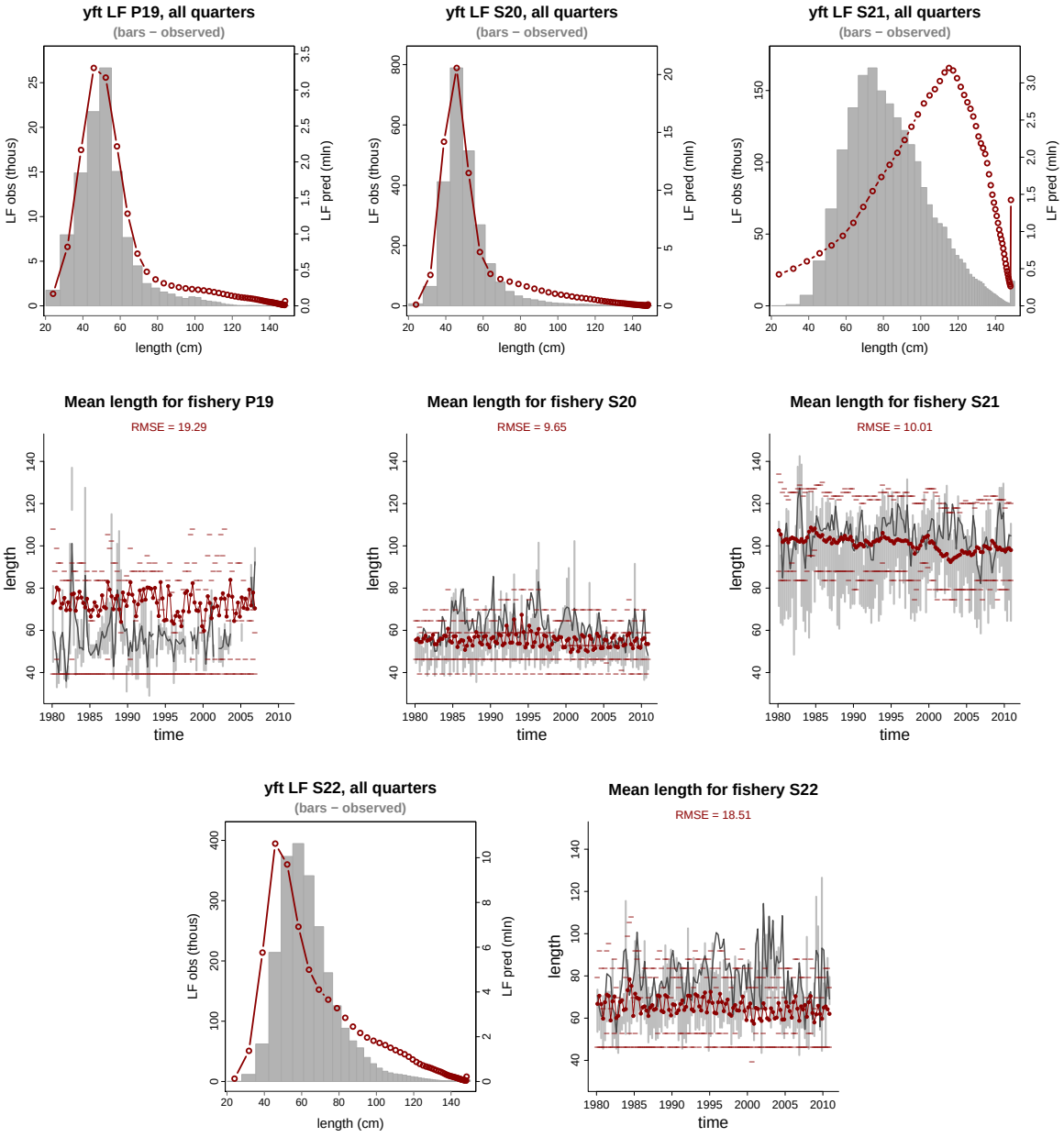

Figure 32: Continued

References

[Boyce *et al.*, 2008] Boyce, D. G., Tittensor, D. P., Worm B. 2008. Effects of temperature on global patterns of tuna and billfish richness. *Mar. Ecol. Prog. Ser.* 355: 267276. doi: 10.3354/meps07237

[Brill, 1994] Brill, R. 1994. A review of temperature and oxygen tolerance studies of tunas pertinent to fisheries oceanography, movement models and stock assessments. *Fisheries Oceanography* 3:3, 204-216.

[Cayre, 1991] Cayre, P. 1991 Behavior of yellowfin tuna (Thunnus albacares) and skipjack tuna (Katsuwonus pelamis) around fish aggregating devices (FADs) in the Comoros Islands as determined by ultrasonic tagging. Aquat Living Resour 4:112

[Faugeras and Maury, 2005] Faugeras, B. Maury, O. 2005. An advection-diffusion-reaction population dynamics model combined with a statistical parameter estimation procedure: application to the Indian skipjack tuna fishery. *Mathematical biosciences and engineering* 2: 4, 1-23.

[Graham and Dickson, 2004] Graham, J. B., Dickson, K. A. 2004. Tuna comparative physiology. *The Journal of Experimental Biology* 207: 4015-4024. doi:10.1242/jeb.01267

[Itano and Holland, 2000] Itano D. G., Holland, K. N. 2000. Movement and vulnerability of bigeye (Thunnus obesus) and yellowfin tuna (*Thunnus albacares*) in relation to FADs and natural aggregation points. *Aquat. Living Resour.* 13: 213223.

[Itano, 2000] Itano, D.G. 2000. The reproductive biology of yellowfin tuna (Thunnus albacares) in Hawaiian waters and the western tropical Pacific Ocean: project summary. SOEST 00-01 JIMAR Contribution 00-328. Pelagic Fisheries Research Program, JIMAR, University of Hawaii.

[Langley *et al.*, 2011] Langley, A., Hoyle, S., Hampton, J. 2011. Stock assessment of yellowfing tuna in the Western and Central Pacific ocean. WCPFC-SC7-2011/SA- WP-03. 9-17 August 2011 Pohnpei, Federated States of Micronesia.

[Lehodey *et al.*, 2009] Lehodey P., Senina I. 2009. An update of recent developments and applications of the SEAPODYM model. 5th Regular Session of the Scientific Committee of the Western Central Pacific Fisheries commission, WCPFC-SC5-2009/EB-WP-10.

[Lehodey *et al.*, 1997] Lehodey, P., Bertignac, M., Hampton, J., Lewis, A., Picaut, J. 1997. El Niño Southern Oscillation and tuna in the western Pacific. *Letters to Nature.* 389, 715-718.

[Lehodey, 2001] Lehodey, P. 2001. The pelagic ecosystem of the tropical Pacific Ocean: dynamic spatial modeling and biological consequences of ENSO. *Progress in Oceanography.* 49, 439-468.

[Lehodey *et al.*, 2003] Lehodey, P., Chai, F., Hampton, J. 2003. Modelling climate-related variability of tuna populations from a coupled ocean biogeochemical-populations dynamics model. *Fish. Oceanogr.* 12: 4/5, 483-494.

[Lehodey, 2004a] Lehodey, P. 2004a. A Spatial Ecosystem And Populations Dynamics Model (SEAPODYM) for tuna and associated oceanic top-predator species: Part I Lower and intermediate trophic components. 17th meeting of the Standing Committee on Tuna and Billfish, Majuro, Republic of Marshall Islands, 9-18 Aug. 2004, Oceanic Fisheries Programme, Secretariat of the Pacific Community, Noumea, New Caledonia, Working Paper: ECO-1: 26 pp. http://www.spc.int/OceanFish/Html/SCTB/SCTB17/ECO-1.pdf

[2004b] Lehodey, P. 2004b. A Spatial Ecosystem And Populations Dynamics Model (SEAPODYM) for tuna and associated oceanic top-predator species: Part II Tuna populations and fisheries. 17th meeting of the Standing Committee on Tuna and Billfish, Majuro, Republic of Marshall Islands, 9-18 Aug. 2004, Oceanic Fisheries Programme, Secretariat of the Pacific Community, Noumea, New Caledonia, Working Paper: ECO-2: 36 pp. http://www.spc.int/OceanFish/Html/SCTB/SCTB17/ECO-2.pdf

[Lehodey and Leroy, 1999] Lehodey, P. and B. Leroy. 1999. Age and growth of yellowfin tuna (*Thunnus albacares*) from the western and central Pacific Ocean as indicated by daily growth increments and tagging data. WP YFT-2, SCTB 12, Papeete, French Polynesia, 16-23 June 1999.

[Lehodey et al, 2014] Lehodey, P., Senina, I., Titaud, O., Calmettes, B., Conchon, A., Dragon, A., Nicol, S., Caillot, S., Hampton, J., Williams, P. 2014. Project 62: SEAPODYM applications in WCPO. WCPFC-SC10-2014/EB-WP-02. 6-14 August, Majuro, Republic of the Marshall Islands.

[Morel and Berthon, 1989] Morel, A, J-F Berthon. 1989. Surface pigments, algal biomass profiles, and potential production of the euphotic layer: Relationships reinvestigated in view of remote-sensing applications. *Limnol. Oceanogr.*, Volume 34: 1545-1562.

[Nicol et al, 2014] Nicol,S., Dessert, M., Gorgues, T., Aumont, O., Menkes, C., P. Lehodey. 2014. Progress report on climate simulations. WCPFC-SC10-2014/EB-IP-02. S.

[Otter Research Ltd, 1994] Otter Research Ltd. 1994. Autodif: a C++ array extension with automatic differentiation for use in nonlinear modeling and statistics. Otter Research Ltd: Nanaimo, Canada.

[Schaefer *et al*, 2011] Schaefer, K. M., Fuller, D. W. Block, B. A. 2011. Movements, behaviour, and habitat utilization of yellowfin tuna (*Thunnus albacares*) in the Pacific Ocean off Baja California, Mexico, determined from archival tag data analyses, including unscented Kalman filtering. *Fisheries Research* 112: 22 - 37.

[Senina *et al.*, 2008] Senina I.N., Sibert, J.R., Lehodey P. 2008. Parameter estimation for basin-scale ecosystem-linked population models of large pelagic predators: Application to skipjack tuna. *Progress in Oceanography* 78, 319-335.

[Sibert *et al.*, 1999] Sibert, J.R., Hampton, J., Fournier, D.A., Bills, P.J. 1999. An advection-diffusion-reaction model for the estimation of fish movement parameters from tagging data, with application to skipjack tuna (*Katsuwonus pelamis*). *Can. J. Fish. Aquat. Sci.* 56, 925-938.

[Sibert *et al.*, 2006] Sibert, J., Hampton, J., Kleiber, P., Maunder, M. 2006. Biomass, Size, and Trophic Status of Top Predators in the Pacific Ocean. Science 314: 1773-1776.

[Sibert and Hampton, 2003] Sibert, J., Hampton, J. 2003. Mobility of tropical tunas and the implications for fishery management. *Marine Policy* 27: 87-95.

[SPC Yearbook 2012] Tuna Fisheries Yearbook. 2012. Western and Central Pacific Fisheries Commission, Pohnpei, Federated States of Micronesia. 148 pp.

[Wexler *et al.*, 2011] Wexler J, Margulies D, Scholey V. 2011. Temperature and dissolved oxygen requirements for survival of yellowfin tuna, Thunnus albacares, larvae. J Exp Mar Biol Ecol 404:6372.

[Williams and Terawasi, 2014] Williams P., Terawasi P. (2014). Overview of tuna fisheries in the Western Central Pacific Ocean, including economic conditions - 2013. 10th Regular Session of the Scientific Committee of the Western Central Pacific Fisheries commission Majuro, Republic of the Marshall Islands, 6-14 August 2014. WCPFC-SC10-2014/GN WP-1.

[Yamanaka, 1990] Yamanaka, K.L. 1990. Age, growth and spawning of yellowfin tuna in the southern Philippines. IPTP. IPTP Working Paper 21, 1-87.